



TECHNICAL UNIVERSITY OF CRETE
SCHOOL OF ENVIRONMENTAL ENGINEERING
POSTGRADUATE PROGRAM:
“ENVIRONMENTAL AND SANITARY ENGINEERING”
MASTER THESIS

Sediment Transport in the Koiliaris River

Nerantzaki Sofia

Supervisor: Nikolaos P. Nikolaidis (Professor T.U.C.)

Examining Board: George P. Karatzas (Professor T.U.C.) and

Ioannis Sibetheros (Professor Technological Educational Institute Of Athens)

Chania
4/28/2014

ACKNOWLEDGMENTS

I would never have been able to finish my dissertation without the guidance of my committee members, help from friends, and support from my family.

Foremost, I would like to express my sincere gratitude to my supervisor. Professor Nikolaos P. Nikolaidis for the continuous support on my study and research, for his patience, motivation, enthusiasm, and immense knowledge. His guidance helped me throughout the research and writing of this thesis. Additionally, I am grateful for the financial support he provided me throughout the study.

I would also like to thank the member of the advisory committee Professor Ioannis A. Sibetheros for his constructive guidance and the excellent cooperation throughout this study.

In addition, I would like to thank the member of the advisory committee Professor Georgios P. Karatzas for the mood to study and evaluate this thesis and for the disposal of valuable time to participate in the examination.

Special thanks to my colleague and Ph.D. candidate, George Giannakis, for the time he spent driving me to the field and for the effort he put helping me with the measurements when conditions were difficult, and mainly for his advice and guidance every time I faced difficulties throughout my research.

I would also like to thank Ph.D. candidate Dionissis Efstathiou for the help he provided me with computer programs and data analysis and for his insightful suggestions.

Last but not least, I would like to thank my family for their patience and support through all these years.

This work is part of a THALES project (CYBERSENSORS - High Frequency Monitoring System for Integrated Water Resources Management of Rivers). The Project has been co-financed by the European Union (European Social Fund – ESF) and Greek national funds through the Operational Program "Education and Lifelong Learning" of the National Strategic Reference Framework (NSRF) - Research Funding Program: Thales. Investing in knowledge society through the European Social Fund.

CONTENTS

ABSTRACT.....	viii
ΠΕΡΙΛΗΨΗ.....	x
1. INTRODUCTION	1
2. THEORETICAL BACKGROUND.....	5
2.1 BASIC CONCEPTS	5
2.1.1 Generally about river solids	5
2.1.2 Types of Sediment Transport.....	5
2.1.3 Issues associated with sediment transport in rivers	7
2.1.4 Erosion processes.....	8
2.1.5 Particle size	10
2.1.6 Suspended Sediment and temporary rivers.....	11
2.1.7 Suspended matter and turbidity	12
2.2 METHODS	14
2.2.1 Measuring Suspended Sediment.....	14
2.2.2 Techniques for automated sampling of suspended sediments	22
2.2.3 Turbidity in automated water sampling	25
2.3 MODELING	26
2.3.1 Review of Models for Sediment Transport and Erosion	26
2.3.2 The SWAT model.....	30
3. CASE STUDY	33
3.1.1 Koiliaris River Basin.....	33
3.1.2 Peculiarity of Koiliaris Watershed.....	35
3.1.3 Sediment transport in the Koiliaris River	35
4. METHODOLOGY	39
4.1 INTRODUCTION	39

4.2 SAMPLING AND MONITORING.....	40
4.2.1 Grab Sampling	40
4.2.2 Limitations from Grab Sampling and suggested method	41
4.2.3 System Architecture.....	41
4.3 SUSPENDED SEDIMENT ANALYSIS	45
4.3.1 Grain Size Analysis.....	45
4.3.2 Geochemical Analysis	48
4.3.3 Turbidity – suspended sediment concentration curve.....	49
4.4 MODELING	51
4.4.1 Augmented SWAT Model	51
4.4.2 Model Input and Data Processing	52
4.4.3 Sediment Equations	54
4.4.4 Erosion Parameters	55
4.4.5 Sediment Routing Parameters	58
4.4.6 Discharge simulation	59
4.4.7 Suspended Sediment Concentration Simulation.....	59
5. RESULTS	61
5.1 PRELIMINARY RESULTS OF THE SEDIMENT TRAP.....	61
5.2 SUSPENDED SEDIMENT ANALYSIS	63
5.2.1 Grain Size Analysis.....	63
5.2.2 Geochemical Analysis	65
5.2.3 Turbidity – suspended sediment concentration curve.....	68
5.3 SWAT MODELING	69
5.3.1 Discharge simulation	69
5.3.2 Suspended sediment simulation	70
5.3.3 Erosion and sediment export.....	71

6	CONCLUSIONS.....	78
	References.....	81

ABSTRACT

This work presents a study of sediment transport in a complex Mediterranean watershed (i.e. the Koiliaris River Basin of Crete) consisting of temporary flow tributaries and karstic springs. Monitoring of suspended sediment concentration in such watersheds is of utmost importance due to first flash events, when large quantities of sediments and pollutants are carried downstream. Up to now, the estimation of river suspended sediment was carried out by laboratory filtration of grab water samples. This technique provides only a rough estimation of the sediment transport. To overcome this, as well as the lack of representative sediment transport data during extreme flow events (e.g. flash floods), an automated sediment sampling device (Sediment Trap), which allows for flow weighted sampling, using turbidity and water level as a trigger for the initiation, has been developed and is presented in this study. The device is undergoing testing to ensure that it can provide accurate estimates of sediment yield, especially during a flash flood event. Field measurements of turbidity were correlated with suspended solids concentrations derived from grab sampling, and an empirical curve between turbidity and suspended sediment concentration was developed. In addition, X-Ray Fluorescence (XRF) analysis was carried out to determine the chemical characterization of the samples, for a comprehensive understanding of the sediments, and the grain size distribution was determined by a laser diffraction particle size analyzer. The automated system will be used to collect data for the calibration of model simulations of the hydrology and sediment transport of the Koiliaris River watershed. Specifically, both daily flow data (2005-2014) and monthly sediment concentration data (2011-2014) were used to calibrate the Soil and Water Assessment Tool (SWAT) model, designed to simulate the hydrology, sediment yield and water quality of ungauged watersheds, augmented with a karst flow model in order to simulate the contribution of the extended karst to the spring discharge in the basin. The results showed good agreement between observed and model values for both flow and sediment concentration.

ΠΕΡΙΛΗΨΗ

Στην εργασία αυτή παρουσιάζεται η μελέτη στερεομεταφοράς σε μια σύνθετη μεσογειακή υδρολογική λεκάνη (τη λεκάνη απορροής του ποταμού Κοιλιάρη στην Κρήτη) που αποτελείται από προσωρινούς παραποτάμους και καρστικές πηγές. Η παρακολούθηση της συγκέντρωσης αιωρούμενων στερεών σε τέτοιες λεκάνες απορροής είναι αναγκαία, λόγω του φαινομένου των «επεισοδιακών πλημμυρών», κατά το οποίο μεταφέρονται κατάντη μεγάλες ποσότητες ιζημάτων και ρυπαντών. Μέχρι τώρα, η εκτίμηση των αιωρούμενων στερεών για τον ποταμό του Κοιλιάρη πραγματοποιούνταν στο εργαστήριο με διήθηση των δειγμάτων που λαμβάνονταν στο πεδίο με το χέρι. Η τεχνική αυτή παρέχει όμως μόνο προσεγγιστική εκτίμηση για τη στερεομεταφορά στο ποτάμι. Για να ξεπεραστεί αυτό, καθώς και η έλλειψη αντιπροσωπευτικών δεδομένων στερεοπαροχής κατά τη διάρκεια ακραίων γεγονότων ροής (π.χ. πλημμύρες), έχει αναπτυχθεί και παρουσιάζεται εδώ μια αυτοματοποιημένη συσκευή δειγματοληψίας αιωρούμενων στερεών (Παγίδα Ιζημάτων), η οποία πραγματοποιεί δειγματοληψία ανάλογη της ροής, χρησιμοποιώντας μετρήσεις θολερότητας και στάθμης σαν έναυσμα. Η συσκευή υποβάλλεται σε δοκιμές για να διασφαλιστεί ότι μπορεί να παρέχει ακριβείς εκτιμήσεις της στερεοπαροχής, ειδικά κατά τη διάρκεια πλημμυρών. Οι μετρήσεις θολερότητας από το πεδίο συσχετίστηκαν με τις συγκεντρώσεις αιωρούμενων στερεών από τις δειγματοληψίες που γίνονταν χειροκίνητα και αναπτύχθηκε έτσι εμπειρική καμπύλη μεταξύ θολερότητας και συγκέντρωσης αιωρούμενων στερεών. Επιπλέον, διεξήχθη ανάλυση Φθορισμού Ακτίνων Χ (X-Ray Fluorescence analysis) για να προσδιοριστεί ο χημικός χαρακτήρας των δειγμάτων, με σκοπό την πλήρη κατανόηση των στερεών, ενώ η κατανομή του μεγέθους των κόκκων προσδιορίστηκε με συσκευή περίθλασης λείζερ. Το αυτοματοποιημένο σύστημα θα χρησιμοποιηθεί για τη συλλογή δεδομένων με στόχο τη βαθμονόμηση μοντέλου προσομοίωσης της υδρολογίας και της στερεομεταφοράς της λεκάνης του ποταμού Κοιλιάρη. Συγκεκριμένα, ημερήσια δεδομένα παροχής (2005-2014) και μηνιαία δεδομένα συγκέντρωσης αιωρούμενων στερεών (2011-2014) χρησιμοποιήθηκαν για τη βαθμονόμηση του μοντέλου SWAT (Soil and Water Assessment Tool – Εργαλείο Εκτίμησης Εδαφών και Νερού), σχεδιασμένο για την προσομοίωση της υδρολογίας, της παραγωγής ιζημάτων και της ποιότητας του νερού, επαυξημένου με ένα καρστικό μοντέλο ροής για την προσομοίωση της συμβολής του εκτεταμένου καρστ στην παροχή της πηγής στη λεκάνη. Τα αποτελέσματα έδειξαν ότι οι τιμές του μοντέλου συμφωνούν με τις παρατηρημένες τόσο για την περίπτωση της παροχής όσο και της συγκέντρωσης αιωρούμενων στερεών.

1. INTRODUCTION

Sediments play an important role in elemental cycling in the aquatic environment. They are responsible for transporting a significant proportion of many nutrients and contaminants. Sediment transport in rivers is associated with a wide variety of environmental and engineering issues. The study of river suspended sediments is becoming more important, nationally and internationally, as the need to assess fluxes of nutrients and contaminants to lakes and oceans, or across international boundaries, increases.

One of the most serious environmental problems is erosion and the consequent loss of topsoil. Although erosion is a natural phenomenon, the rate of soil loss is greatly increased by poor agricultural practices which result, in turn, in increased suspended sediment loads in freshwaters.

In order to protect surface water resources and optimize their use, soil loss must be controlled and minimized. This, in turn, demands an understanding of sediment transport and appropriate methods for measuring sediment load and movement. Recognition of the importance of sediments and their use in monitoring and assessment programs is increasing and methods are constantly being refined. Suspended matter concentrations should be measured along with other hydrological variables. Knowledge of the sources and the processes which determine the delivery rate of suspended sediments to stream channels is required to formulate sediment budgets, to enhance the performance of simulation models, and to make informed management decisions about the effectiveness of land use and pollution control strategies (Hicks et al., 2000).

Quantification of sediment fluxes through the development of new measuring devices is of utmost importance, especially in the Mediterranean region, which is characterized by a unique micro-climate and a complex geologic and geomorphologic environment caused by its position in the Alpine orogenesis belt. Unique features of the climatic and geomorphologic regime of the region are the “temporary rivers”. Temporary river hydrographs are flashy and exhibit characteristic response times ranging from minutes to hours such as those experienced during first flash and storm events. During dry periods, temporary rivers have no flow and their riverbeds are completely dry. On the other hand, in temporary environments the river bed is expanding in the winter during the flooding events and is contracting during the dry

period. During the first flash and the following rain events, discharge, sediments, and nutrients concentrations are high compared to baseflow conditions.

This study aims to provide an overview of a system which concerns suspended sediment measurements in the Koiliaris river, in Crete, Greece. Since the available sediment concentration data from grab samples in Koiliaris were limited to low concentration values and there were no data available during flood conditions, an automatic suspended sediment sampler has been developed. The automatic sampler works as follows: water is pumped during storm events and the pump rotation is proportional to the stage, allowing for a flow weighted sampling. Sediment sampling is initiated automatically when water surpasses a certain level, and/or when turbidity surpasses a certain threshold. The water then passes through a sediment trap that captures the sediment. The sediment sampler is currently undergoing testing to ensure its operational robustness, particularly under harsh environmental conditions. Field measurements of turbidity are also correlated with suspended solids concentrations derived from grab sampling, and an empirical curve between turbidity and suspended sediment concentration is developed, in an attempt to define the operating conditions. In addition, X-Ray Fluorescence (XRF) analysis was carried out to determine the chemical characterization for a comprehensive understanding of the sediments and the grain size distribution was determined by a laser diffraction particle size analyzer.

The system deployment at Koiliaris River will be used to collect data for the calibration of model simulations of the hydrology and sediment transport of the Koiliaris River watershed, as well as for the modeling of bank erosion. Specifically, daily flow data (2005-2014) and monthly sediment concentration data (2011-2014) were used to calibrate discharge and sediment concentration simulations by the modified Soil and Water Assessment Tool (SWAT) model. The latter is designed to simulate the hydrology, sediment yield and water quality of ungauged watersheds, but for the Koiliaris watershed case it is augmented with a karst flow model in order to simulate the contribution of the extended karst to the spring discharge in the Koiliaris basin.

The sediment sampler is an important component of the Cybersensors infrastructure. The research project “Cybersensors” (High Frequency Monitoring System for Integrated Water Resources Management of Rivers) aims to develop and implement an intelligent, integrated environmental data collection system, combining high frequency monitoring and real-time observing systems for the quantification of the hydrologic and geochemical processes that take place in Mediterranean watersheds. The system will utilize optical, pressure and

electrochemical sensors, for the river's physical (i.e. water level, suspended solids, temperature) and chemical parameters (i.e. conductivity, dissolved oxygen, nitrates, pH and heavy metals) monitoring.

2. THEORETICAL BACKGROUND

2.1 BASIC CONCEPTS

2.1.1 Generally about river solids

River solids are composed of solid particles of metal and organic material that are transported with water. Most sediment in surface waters derive from surface erosion and comprises of a mineral component, originating from the erosion of the parent material, and of an organic component from soil-forming processes (including biological and microbiological production and decomposition). An additional organic component may be added by biological activity within the water body. In river systems, the percentage of transported solids is controlled by both the capacity of the flow and the abundance of solids. For the purposes of aquatic monitoring, sediment can be classified as deposited or suspended. Deposited sediment is that found on the bed of a river or lake. Suspended sediment is that found in the water column where it is being transported by water. Suspended sediment is also referred to as suspended matter, particulate matter or suspended solids. Generally, the term suspended solids refers to mineral and organic solids, whereas suspended sediment is restricted to the mineral fraction of the suspended solids load. The “suspended solids” or “suspended sediments” may include material collected from the river bed (bed material in suspension) and materials that are washed into the river from the surrounding areas (wash load). The wash load is usually finer than the bed material in suspension. On the other hand, the “bed load” includes larger particles of sediment transported by the river bed by rolling, sliding or bouncing. Most rivers carry sediments in each of these forms of load, according to the flow conditions. (Bartram and Ballance, 1996)

2.1.2 Types of Sediment Transport

Sediment transport is a direct function of water movement. During transport in a water body, sediment particles become separated into three categories: suspended material which includes silt, clay and sand; the coarser, relatively inactive bedload and the saltation load (Bartram and Ballance, 1996).

Suspended load comprises of sand, silt and clay-sized particles that are held in suspension because of the turbulence of the water. Suspended load is the result of material eroded by hydraulic action at the stream surface bordering the channel as well as erosion of the channel

itself. Suspended load accounts for the majority of stream load (Strahler and Strahler, 2006). The suspended load is further divided into the wash load which is generally considered to be the silt and clay-sized material ($< 62 \mu\text{m}$ in particle diameter) and is often referred to as “fine-grained sediment”. The wash load is mainly controlled by the supply of this material (usually by means of erosion) to the river. The amount of sand ($>62 \mu\text{m}$ in particle size) in the suspended load is directly proportional to the turbulence and mainly originates from erosion of the bed and banks of the river. In many rivers, suspended sediment (i.e. the mineral fraction) forms most of the transported load.

Bedload is stony material, such as gravel and cobbles, that moves by rolling along the bed of a river because it is too heavy to be lifted into suspension by the current of the river. Bedload is especially important during periods of extremely high discharge and in landscapes of large topographical relief, where the river gradient is steep. Measurement of bedload is extremely difficult. Despite many years of experimentation, sediment-monitoring agencies have so far been unable to devise a standard sampler that can be used without elaborate field calibration or that can be used under a wide range of bedload conditions. Even with calibration, the measurement error can be very large due to the immense difficulty with representative sampling of the range of sizes of particles in transit as bedload in many rivers.

Saltation load is a term used by sedimentologists to describe material that is transitional between bedload and suspended load. Saltation means “bouncing” and refers to particles that are light enough to be picked off the river bed by turbulence but too heavy to remain in suspension and, therefore, sink back to the river bed. Saltation load is never measured in operational hydrology.

The three forms of sediment transport are presented in Figure 2.1.

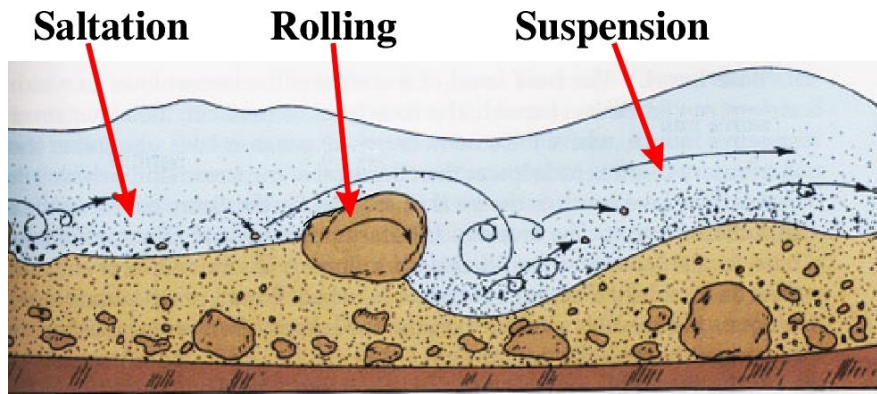


Figure 2.1: Types of sediment transport (<http://www.geol.umd.edu/~piccoli/100/CH12.htm>)

2.1.3 Issues associated with sediment transport in rivers

Sediment transport in rivers is associated with a wide variety of environmental and engineering issues which are outlined in Table 2.1. The study of river suspended sediments is becoming more important, nationally and internationally, as the need to assess fluxes of nutrients and contaminants to lakes and oceans, or across international boundaries, increases.

One of the most serious environmental problems is erosion and the consequent loss of topsoil. Although erosion is a natural phenomenon, the rate of soil loss is greatly increased by poor agricultural practices which result, in turn, in increased suspended sediment loads in freshwaters. Good environmental practice in agriculture, which may include contour ploughing and terracing, helps to protect against soil loss and against contamination of surface waters.

Reservoir siltation is another major problem that water users downstream of areas of heavy soil run-off may have to deal with, as they may have to remove suspended sediment from their water supplies or suffer a reduction in the quantity of water available. The rapid reduction in the storage capacity of reservoirs due to siltation is a major sediment-related problem world-wide. Moreover, the low availability of water for irrigation from the reservoir leads to more intensive land use and increased soil erosion. Desertification (impoverishment of vegetative cover and loss of soil structure and fertility) may also exacerbate the above mentioned effects, whether anthropogenic or climatic in origin. In addition, gradual enrichment of reservoir waters with nutrients (some of which also arise from agricultural practices) leads to enhanced production and increased sedimentation of organic material originating from the water column (from decaying plankton) or littoral zones (from decaying

macrophytes). Consequently, the rate of reservoir siltation often greatly exceeds that predicted during design.

Table 2.1: Issues associated with sediment transport in rivers (Bartram and Ballance, 1996)

Sediment Size	Environmental Issues	Associated engineering issues
Silts and clays	Erosion, loss of topsoil in agricultural areas; gullyng	
	High sediment loads to reservoirs	Reservoir siltation
	Chemical transport of nutrients of nutrients, metals, and chlorinated organic compounds	Drinking water supply
	Accumulation of contaminants in organisms at the bottom of the food chain (particulate feeders)	
Sand	Silting of fish spawning beds and disturbance of habitats (by erosion or siltation) for benthic organisms	
	River bed and bank erosion	River channel deposition: navigation problems
	River bed and bank erosion Habitat distrurbance	Sedimentation in reservoirs
Gravel	Channel instability when dredged for aggregate	Instability of river channel leads to problems of navigation and flood - control
	Habitat disturbance	

2.1.4 Erosion processes

The process of erosion follows three stages: detachment, transport and deposition. Detachment of sediment from the soil surface is the result of raindrop impact in combination with overland flow. Rainfall detachment is caused by the locally intense shear stresses generated at the soil surface by raindrop impact. Likewise, overland flow causes a shear stress to the soil surface which, if it exceeds the cohesive strength of the soil (critical shear stress) results in sediment detachment. In different situations, the major processes leading to sediment detachment will differ (Merritt et al, 2003). There are four main types of erosion processes: sheet, rill, gully, and in-stream erosion (Figures 2.2 and 2.3).

Sheet erosion refers to the uniform detachment and removal of soil, or sediment particles from the soil surface by overland flow or raindrop impact evenly distributed across a slope. Together with rill erosion, sheet erosion is often classified as “overland flow” erosion, detaching sediment from the soil surface profile only.

Rill erosion occurs when water moving over the soil surface flows along preferential pathways forming an easily recognizable channel. These rills are generally small erosion features, and have been defined by Loch and Silburn (1996) as being flow channels that can be obliterated by tillage. Rill initiation is controlled by the cohesive strength of the soil and the shear forces exerted on the soil. Flow in rills acts as a transporting agent for the removal of sediment downslope from rill and interill sources, although if the shear stress in the rill is high enough the rill flow may also detach significant amounts of soil (Merritt et al, 2003).

Gully erosion, in contrast to rill erosion, describes channels of concentrated flow that are too deep to be obliterated by cultivation (Rose, 1993; Loch and Silburn, 1996). Gully flows differ from sheet and rill flows in that raindrop impact is not an important factor in terms of flow resistance or in sediment particle detachment (Bennett, 1974). Gully development is considered to be controlled by thresholds, as with rills, although these thresholds have been related to slope and catchment area rather than flow erosivities (Loch and Silburn, 1996).

In-stream erosion involves the direct removal of sediment from stream banks (lateral erosion) or the stream bed. Sediment also enters the stream due to slumping of the stream bank resulting from bank erosion undercutting the stream bank. During high flow periods, a large proportion of the sediment that is transported through the stream network can originate from the stream channel. The potential exists to lump stream bank erosion processes with gully erosion for description by considering either as a specific form of the other.

These erosion types do not necessarily occur in isolation from one another. They are influenced by the landscape factors as well as rainfall characteristics.

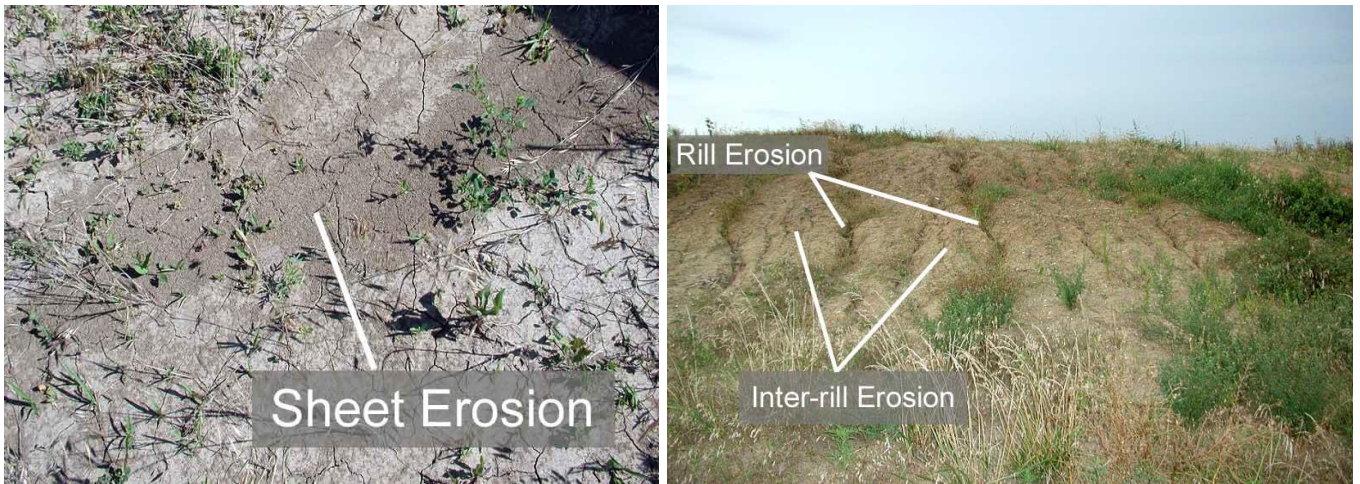


Figure 2.2: a) Sheet Erosion b) Rill Erosion (Plant & Soil Sciences eLibrary, image by M. Mamo, Labels added by UNL)



Figure 2.3: a) Gully Erosion (Plant & Soil Sciences eLibrary, image by NRCS) b) In – stream Erosion (geograph.org.uk)

2.1.5 Particle size

Knowledge of the size gradient of particles that make up suspended load is a prerequisite for understanding the source, transportation and, in some cases, environmental impact of sediment. Although particles of sizes ranging from fine clay to cobbles and boulders may exist in a river, suspended load will rarely contain anything larger than coarse sand, and in many rivers 50-100 percent of the suspended load will be composed only of silt and clay-sized particles (< 62 μm). The size of particles is normally referred to as their diameter.

Particle size is determined by passing a sample of sediment through a series of sieves, each successive sieve being finer than the preceding one. The fraction remaining on each sieve is weighed and its weight expressed as a percentage of the weight of the original sample. The cumulative percentage of material retained on the sieves is calculated and the results are plotted against the representative mesh sizes of the sieves. A series of eight sieves can be used for sediment analysis, with mesh sizes from 1.25 mm to 63 μm or less.

Clay particles are plate – like in shape and have a maximum dimension of about 4 μm . Silt particles, like sand, have no characteristic shape; their size is between those of clay and sand with diameters ranging from 4 μm to 62 μm . Since the smallest mesh size of commercially available sieves is about 40 μm , the sizes of clay and small silt particles cannot be determined by sieving, and other techniques are used instead (See Chapter 4.3.1).

The boundary between sand and silt (62 μm) separates coarse-grained sediments (sand and larger particles) from fine-grained sediments (silt and clay particles). Coarse-grained sediments are non-cohesive, whereas fine-grained sediments are cohesive, i.e. the particles will stick to one another as well as to other materials. Sedimentology and water quality programs have adopted a convention that considers particulate matter to be larger than 0.45 μm in diameter; anything smaller is considered to be dissolved. This boundary is not entirely valid because clay particles and silt can be much smaller than 0.45 μm .

There is no universally accepted scale for the classification of particles according to their sizes. The Wentworth Grade Scale as well as the International Grade Scale is commonly used. There are minor differences between the two scales and it is, therefore, important to note which scale has been selected and to use it consistently.

2.1.6 Suspended Sediment and temporary rivers

The Mediterranean region is characterized by its own micro-climate and a complex geologic and geomorphologic environment caused by its position in the Alpine orogenesis belt. Unique features of the climatic and geomorphologic regime of the region are the “temporary rivers” (Tzoraki et al., 2007). The term “temporary river” refers to all intermittent, ephemeral and episodic streams. Temporary river watersheds constitute 30% of the Mediterranean region and at least 42% of the Greek territory (Tzoraki and Nikolaidis, 2007).

Temporary river hydrographs are flashy and exhibit characteristic response times ranging from minutes to hours such as experienced during first flash and storm events (Tzoraki et al., 2007). When high rainfall intensities fall upon crusted soil after long periods without precipitation, Horton-type overland flow is induced causing very fast response. During a season's first flood a significant remobilization of accumulated debris occurs in a phenomena described as the 'first flash effect'. First flash events transfer large quantities of sediments and pollutants in both urban and rural areas. Compared to perennial flow conditions, temporary rivers deliver most of the annual pollution load during only a few flood events typically lasting a few hours (Moraetis et al., 2010).

A flash flood hydrograph is composed of three major parts. First is a flash flood bore or "wall of water," a front of water typically characterized by increased turbulence, followed by a rising limb with increasing discharge, and lastly a decreasing falling limb. Field observations show that sediment transport rates are elevated in the flood bore and decrease in the rising limb contrary to decreasing discharge.

2.1.7 Suspended matter and turbidity

The type and concentration of suspended matter controls the turbidity of the water. The optical property expressed as turbidity is the interaction between light and suspended particles in water. A minute particle interacts with incident light by absorbing the light energy and then, as if a point light source itself, reradiating the light energy in all directions. This omnidirectional re – radiation constitutes the "scattering" of the incident light. In samples containing suspended solids, the manner in which the sample interferes with light transmittance is related to the size, shape and composition of the particles in the solution and to the wavelength (color) of the incident light.

In situ sensing devices of optical backscattering (See Chapter 2.2.1) use the principle that the mass of material present is proportional to the attenuation or scattering of an incident beam of radiation. The devices use various radiation sources, but the most popular device for this purpose is the optical turbidimeter. There are two main types of commercial turbidimeter. Attenuation turbidimeters measure the loss in intensity of a narrow parallel beam passing through a known pathlength of medium. Nephelometric turbidimeters have the detector aligned at an angle to the beam, and therefore measure scattered light (Gippel, 1995)

Turbidity is affected by the sensor design, the particle size distribution, the particle shape, the composition, and water color (Gippel, 1989). For the same concentration and particle size, organic particles can give attenuation turbidity values two to three times higher than mineral particles (Gippel, 1995). Color-producing dissolved organic substances increase attenuation turbidity but reduce nephelometric turbidity. Infrared turbidimeters are unaffected by water color, but are less sensitive than visible light turbidimeters to scattering from fines.

Gippel (1995) states that adequate relations between field turbidity and sediment concentration can be expected in most situations. At a given river station turbidity can often be related to TSS, especially where there are large fluctuations in suspended matter. Particle size variations are generally small or associated with variations in concentration. Turbidity data should be able to improve estimates based on infrequent measurements of concentration. However, in the presence of so many confounding factors, turbidity should not be used as a substitute for sediment concentration without careful study of the relation between turbidity and suspended load for any proposed monitoring sites. Without accompanying concentration data, there is no assurance in the quality of the estimate's (Lewis, 1996).

Turbidity should be measured in the field but, if necessary, samples can be stored in the dark for not more than 24 hours. The most reliable method of determination uses nephelometry (light scattering by suspended particles) by means of a turbidity meter which gives values in Nephelometric Turbidity Units (NTU). Assuming that the nephelometric turbidimeter has been calibrated to give a linear response to standards (such as formazine) varying only in concentration, the relationship between turbidity (T) and the suspended solids concentration (C) can be described with a linear model, which assumes that the particle size and composition do not systematically vary with respect to concentration, and takes the general form

$$T = aKC \tag{2.1}$$

where K is a characteristic coefficient called the specific turbidity. For nephelometric turbidimeters, $a \leq 1$ and is a function of the concentration of dissolved colored organic matter.

2.2 METHODS

2.2.1 *Measuring Suspended Sediment*

The measurement of suspended sediment concentrations is an important topic that merits continuing research. Accurate measurements of suspended sediment concentration are difficult to obtain, since suspended sediment loads are highly variable in both time and space. In this chapter, methods for measuring suspended sediment concentration and, in some cases, particle – size distribution are described. The operating principles, advantages, and disadvantages of the techniques are discussed (Walling and Horowitz, 2005).

- **Bottle Sampling**

Bottle sampling includes taking a water sample isokinetically by submerging a container in the river flow. The sample is then analyzed in the laboratory and sediment concentration and size distribution are determined, using standard techniques (Guy, 1965). There are point and depth integrating samplers, the use of which allows for isokinetic sampling (Interagency Committee, 1963). Specifically, depth integrating samples are used to sample the water in a vertical section, by lowering the apparatus to the desired level (usually close to the bed) and the raising the sampler back to the surface at the same rate.

Bottle – sampling is an accepted, time tested technique; the majority of the rest of the techniques is calibrated against bottle samplers. The use of depth integrating samplers allows for a full sampling of the entire depth of the stream and the determination of the concentration and size distribution is possible with laboratory techniques. Nevertheless, bottle sampling has poor temporal resolution and there is the need for specialized personnel to be available to take samples, thus the cost of the procedure increases. On the latter, required laboratory analysis is added. Bottle samplers also require an intrusion in the flow, although using streamlined samplers minimizes this effect.

- **Pump Sampling**

In pump sampling, a vacuum is applied to an intake nozzle submerged in the channel and a fluid – sediment sample is taken and stored for laboratory analysis. The intake velocity is matched to the local stream velocity to avoid sample biasing. As mentioned above for the case of bottle sampling, the sediment concentration and size distribution can be determined at the lab by using standard techniques.

Pump sampling is a time – tested technique which provides a reliable method for collecting samples and works well for fine sediments (< 0.062 mm). It is commonly used in automatic samplers, as the programming to take samples at predetermined intervals or at predetermined flows or depths (when coupled with appropriate sensors) is possible. This automation eliminates the need for personnel to be present during sampling. The determination of concentration and size distribution is also possible from laboratory analysis. On the other hand, this method (like bottle – sampling) has poor temporal resolution. Personnel and laboratory analysis also add expense to the sampling. In addition, the amount and size of sediment sampled are dependent on the pump's speed as well as the nozzle's orientation with respect to the flow direction. Finally, pump sampling is flow intrusive; it has been shown, though, that intake velocity will not cause errors greater than 20% as long as the intake velocity is not less than 80% or greater than 200% of the local flow velocity (Nelson & Benedict, 1950).

- Acoustic Methods

The technology for making acoustic measurements of suspended sediment has been available for a number of years and instruments have been developed and applications reported (Young et al., 1982; Hanes et al., 1988; Libicki et al., 1989). The principle under these instruments is the same: A transducer emits a short pulse ($\gg 10\text{ms}$) of high frequency sound (1-5 MHz) towards the measured volume and sediment in suspension directs a portion of this sound back to the transducer (Thorne et al., 1991) (Figure 2.4). When the sediment is of uniform size, the strength of the backscattered signal allows the calculation of sediment concentration. The backscattered strength is related to both particle size and concentration. With the use of multiple frequencies, the investigation of both particle size (Crawford and Hay, 1993) and concentration is possible.

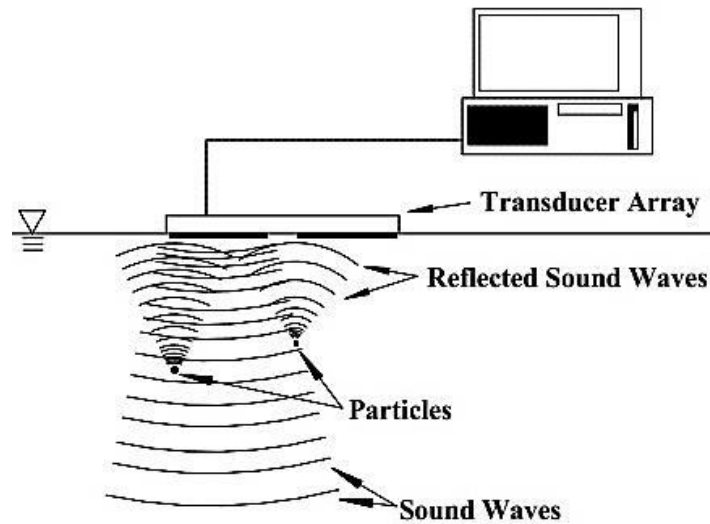


Figure 2.4: Acoustic backscatter (Wren et al. 2000)

Acoustic suspended-sediment measurement offers the ability to non-intrusively measure sediment parameters. The degree of temporal ($\gg 0.1$ s) and spatial ($\gg 1$ cm) resolution is high, thus offering the opportunity to study the mechanics of turbulent sediment transport (Thorne et al., 1994). However, backscattered acoustic signal is difficult to be translated into sediment concentration and size (Hanes et al., 1988). Another problem is the difficulty of creating a calibration apparatus that can maintain a uniform sediment concentration suitable for use in calibrating instruments. In addition, at high particle concentration, attenuation becomes a significant problem.

- Focused Beam Reflectance

In focused beam reflectance measurement, a laser beam focused to a very small spot (< 2 mm) in the sample volume is rotated very quickly (many times per second). As it rotates, the beam encounters particles that reflect a portion of the beam (Figure 2.5). The time of this reflection event is used to determine the sizes of the particles in the path of the laser. This information is used to calculate the volume of a sphere representing the particle (Phillips and Walling, 1995b; Law et al., 1997).

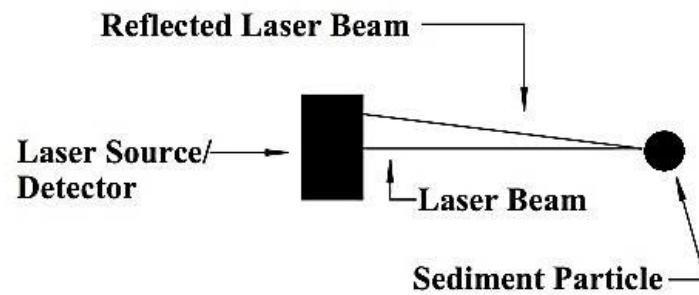


Figure 2.5: Focused beam reflectance (Wren et al. 2000)

Focused beam reflectance has the advantage that there is no particle size dependency since concentration measurements from focused beam reflectance are based on particle size. The instrument has a wide particle measuring range and it is easily portable. However, if particles have little or no reflectance, such as particles high in organic matter, the instrument will work poorly or not at all. In addition, since particle sizes are based on chord lengths, the assumption of sphericity is required. In a situation involving particle shapes that vary drastically from spheres, poor readings may result (Law et al., 1997). Finally, the instrumentation is quite expensive and its nature makes it to be flow intrusive.

- Laser Diffraction

A laser beam is directed into the measured volume and the particles in suspension will scatter, absorb and reflect the beam (Figure 2.6). Then, the scattered laser light, is received by a multi-element photo detector which allows for measurement of the scattering angle of the beam. Particle size can be calculated from knowledge of this angle. However, in the absence of additional information, particle density must be assumed (Agrawal and Pottsmith, 1994).

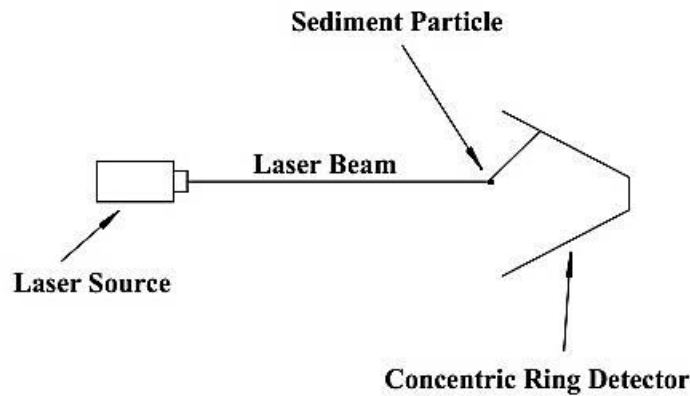


Figure 2.6: Laser Diffraction (Wren et al. 2000)

Particle size dependency is eliminated, since sediment concentration is calculated from size measurements (calculation of the concentration based on the volume of the particles) (Agrawal and Pottsmith, 1994; Riley and Agrawal, 1991; Knight et al., 1991). On the other hand, laser diffraction devices are expensive. They are quite complicated devices that may require specialized training for operation and data interpretation. Also, the particle size measurement is limited to 250 μm and the concentration range to 5000 mg/l. This means that longer focal distances are necessary for measurement of larger particles (Witt and Rüttele, 1996). Finally, since the measuring volume of laser diffraction devices are very close to the instrument, they are flow intrusive.

- Nuclear Measurement

In general, nuclear sediment measurement relies on the attenuation or backscatter of radiation, usually X or gamma rays, by sediment particles. An empirical calibration is used to convert backscatter to concentration. The concentration range is approximately 0.5-12 g/L. The measurement volume will depend on instrument geometry.

Nuclear instruments have the advantage that they have low power consumption so they are well suited when continuous measuring is necessary. They can also be used over a wide range of sediment concentrations (500-12,000 mg/l), and they are not affected by the color of water or by suspended organic matter (Papadopoulos and Ziegler, 1966; Tazioli, 1981; Berke and Rakoczi, 1981).

Radioisotopes are though, by nature, subject to decay, and the source must eventually be replaced (Welch and Allen, 1973) and changing chemical composition of sediments can

affect readings. In addition, the geometry of the gamma backscatter instruments prevents their use in streams less than 1.5 m deep (Berke and Rakoczi, 1981). Low sensitivity is also an important limitation; nuclear instruments are best suited to sediment concentrations above 1000 mg/L (Crickmore et al., 1990).

- Optical Backscatter

In optical backscatter (OBS) sensing, infrared or visible light is directed into the sample volume, where a portion of the light will be backscattered if particles are in suspension. A series of photodiodes positioned around the emitter detects the backscattered signal. The strength of this backscattered signal is used to determine the sediment concentration.

OBS response to varying concentrations of homogeneous sediments is nearly linear (Black & Rosenberg, 1994; Green & Boone, 1993). This linearity extends over a wider range than optical transmission instruments (D & A Instruments, 1991). OBS sensors allow very good spatial and temporal resolution and they are readily available from several manufacturers, providing real-time output as well as the option of remote deployment and data recording. Particle size dependency is the main problem with using OBS (Black & Rosenberg, 1994; Ludwig & Hanes, 1990; Green and Boone 1993; Xu 1997; Kineke and Sternberg 1992; Conner & Devisser 1992). In particular, OBS sensors are more sensitive to smaller particle sizes. When used to record field data over long periods of time, fouling of the sensor face is also a problem. These instruments are also flow intrusive.

- Optical Transmission

In optical transmission sensing, light is directed into the sample volume. Sediment present in the sample volume will absorb and/or scatter a portion of the light. A sensor located opposite the light source allows determination of the degree of attenuation of the light beam. The sediment concentration is determined using empirical calibration information.

Optical transmission instruments have most of the same advantages as optical backscatter instruments. Optical transmission sensors allow very good spatial and temporal resolution and are generally more sensitive to low particle concentrations than OBS instruments. They are readily available from several manufacturers. On the other hand, optical transmission devices exhibit weaknesses similar to OBS devices, although the particle size dependency is somewhat less severe than with OBS (Clifford et al. 1995). The refractive index of the particles also affects transmission devices (Baker and Lavelle, 1984). Optical transmission instruments show a non-linear response to increasing particle concentrations with

disproportionately small changes in output being produced by large changes in sediment concentration in the upper range of the instrument. Finally, these instruments are flow intrusive.

- Spectral Reflectance

This technique is based on the relationship between the amount of radiation, generally in the visible or infrared range, reflected from a body of water and the properties of that water (Figure 2.7). The radiation is measured by a hand held, airborne, or satellite based spectrometer. The size of the measured area is much larger than the other devices discussed here and may range from m^2 to km^2 of the surface of the water body. This technique is better suited to marine environments where large areas are under observation or in other situations where concentration variations over large areas are of interest (Novo et al., 1989). This relationship is dependent on many parameters such as the optical properties of the sediment type, sensor observation angle, solar zenith angle, and the spatial resolution of the measurements

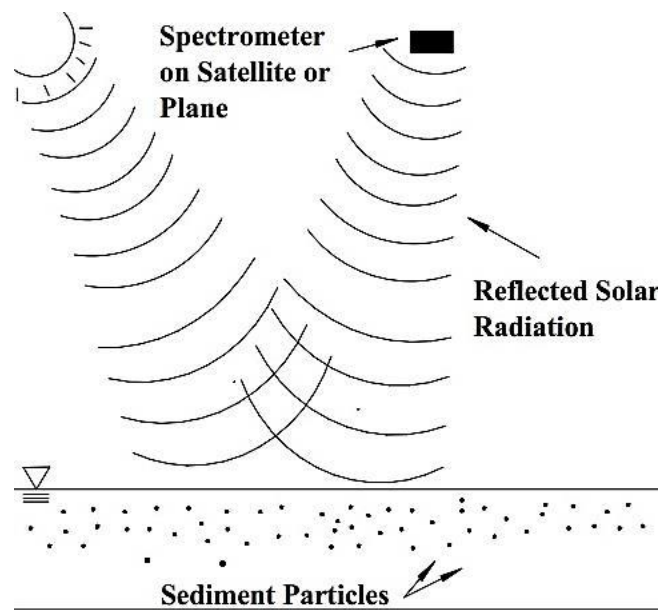


Figure 2.7: Remote spectral reflectance (Wren et al. 2000)

The main advantages of the device is the ability to measure sediment concentrations over broad areas and the ability to detect changes in time. This type of data can be used to identify water bodies with high-suspended-sediment concentrations and allows conservation efforts to be concentrated on areas with significant erosion problems (Ritchie and Schiebe, 1986). However, the resolution provided is poor, and the same stands for the applicability in fluvial

environments. Particle size dependence is also a problem with this method (Novo et al., 1989b).

- Vibrating tube:

Water is routed through a vibrating tube in a stationary housing located either on the stream bank or in the stream. The frequency of the vibration will be affected by the density of the water in the tube and can be used to determine the sediment concentration. However, several other factors such as temperature, debris on the tube walls, and dissolved solids concentration also affect the vibration frequency. All of these must be accounted for to obtain an accurate measurement (Skinner, 1989)

- Differential pressure

A differential pressure transducer may be used to determine differences in the specific weight of sediment bearing water versus water nearer the surface with lower concentrations. This difference in pressure can be used to determine the average suspended sediment concentration between the two inlets of the differential pressure transducer. The size of the measurement volume will depend on the separation of the pressure inlets of the differential transducer. The concentration range is dependent on the sensitivity of the transducer. The hardware for this device is readily available and relatively inexpensive. Changes in temperature gradient, turbulence, and dissolved solids concentration will affect the measurements. (Lewis and Rasmussen, 1996)

- Impact sampler:

The sampler works on the principle of momentum transfer. The impact rate of sediment particles hitting a sensor is measured. The detected impact rate is dependent on the mass, velocity, and angle of particle impact. Few references to this type of device are found in the literature. There are many technical problems with the use of this device in a fluvial environment. (Salkield et al., 1981)

- Video Microscopy

In video microscopy, an underwater video camera films the water-sediment mixture in-situ. This film can be used to visually confirm the nature of the sediment. The film can also be examined by a computer-controlled automated analysis system for determining the size, shape, and number of sediment particles. Some factors in this measuring scheme are the type of lighting used, the sensitivity of the video system, and the method of image processing used

to analyze the samples (Baier and Bechteler, 1996). This method is still undergoing testing, but it has the potential to provide excellent information on the specific nature of sediment particles

Conclusions:

At the present time many options exist for the measurement of sediments suspended in water. All of the techniques reviewed above, however, suffer from limitations that render the techniques inadequate in some environments. The optimal solution for suspended sediment measurement would be a hybrid approach that relies on more than one technique and maintains a manual component.

2.2.2 Techniques for automated sampling of suspended sediments

Automatic sampling methods originate in the mid 80's. The basis of those methods is the use of easy to measure surrogate variables that are monitored with in situ sensing devices. Usual methods propose a data logger programmable to record either stage or flow rate in real time and every time stage (or flow) rise over a certain amount, or on predefined fixed intervals, water specimens are taken from a certain position of the flow depth. In this section, the most common sampling techniques for bottle sampling are described. (Abtew and Powell, 2003)

- Time – proportional discrete sampling

Time – proportional discrete sampling is the process of taking aliquots of samples on fixed time intervals and analyzing each aliquot separately. The load for each time interval can be computed using the Equation 2.2, provided that time – stamped flow data is available for each aliquot. Load can vary with sampling time interval or sampling event based on variation in concentration, flow or both.

$$L_i = C_{ti}V_i \quad (2.2)$$

Where L_i is load for time interval i ; C_{ti} is concentration of aliquot taken during time interval i ; and V_i is volume of flow for time interval i . Total load (L_t) is computed as follows:

$$L_t = \sum_i^t L_i \quad (2.3)$$

High resolution time – discrete sampling can provide “true” constituent load and temporal variation of concentration and flow, provided corresponding data are available. The drawback is that many samples must be analyzed resulting in high cost. An advantage of this sampling scheme is that it is easier to program and operate time – activated auto – samplers, as the date of the last sampling event can be predetermined with most present – day samplers.

- Time proportional discrete composite sampling

Time proportional discrete composite sampling is the process of taking aliquots of samples on a predetermined, equal time interval and compositing at the end of the sampling process to analyze a single composite sample. There is the option to analyze each aliquot or discard some aliquots based on field quality control procedures. The representative concentration (C_t) is:

$$C_t = \frac{\sum_{i=1}^N C_{ti}}{N} \quad (2.4)$$

where N is the number of time intervals or total number of aliquots taken. Load can vary with sample based on variation in concentration, variation of flow or both. An advantage is that it is easier to program and operate time – activated auto – samplers.

- Time – proportional composite sampling

Time – proportional composite sampling is the process of taking aliquots of samples on a fixed time interval and instantly compositing them in a single sample container from which one sub- sample is analyzed. Constituent load is computed using Equation 2.2, provided that total flow volume is also measured. As a result of mixing aliquots, the relationship of flow and concentration is not maintained. The primary advantage of time – composite sampling is the reduced analytic cost due to analysis of a single composite sample. A secondary advantage is that it is easier to program and operate time – activated auto – samplers as the date of the last sampling event can be predetermined.

- Flow – proportional discrete sampling

Flow – proportional discrete sampling is the process of taking aliquots of samples on a fixed flow volume interval (sampling trigger volume) and analyzing each aliquot separately. Load can vary with sample only based on variation in concentration. The load for each aliquot (L_i) can be computed as follows:

$$L_i = C_{fi} \Delta V \quad (2.5)$$

Where C_{fi} is concentration of sampling aliquot i ; ΔV is the sampling trigger volume or the volume of flow that passes through, before each discrete sample is taken. Representative concentration (C_f) is computed with Equation 2.7. Total flow volume (V_t) is computed as follows and N is the number of discrete samples:

$$V_t = N \cdot \Delta V \quad (2.6)$$

Flow – proportional discrete sampling with optimum sampling trigger volume can provide “true” constituent load and temporal variation of concentration and flow. The major challenges are determining sampling trigger volume for variable – flow in remote canals where flow is not known *a priori*. Another disadvantage is that the samples to be analyzed are many and the costs can be high.

- Flow – proportional discrete composite sampling

Flow – proportional discrete composite sampling is the process of taking aliquots on a fixed flow volume interval (sampling trigger volume) and mixing the discrete samples to produce a composite sub – sample. Aliquots are taken at the end of each sampling trigger volume and composited to after the sample collection process is completed, to produce a single sub – sample that will be analyzed. Constituent load is computed using Equation 2.2 and representative concentration (C_f) is expressed by the following equation

$$C_f = \frac{\sum_{i=1}^N C_{fi}}{N} \quad (2.7)$$

The major challenge in determining sampling trigger volume for variable – flow, in remote canals, is that the flow rate is *a priori* unknown for the sampling period. There is also the need to implement cost – effective sampling instrumentation and a sampling scheme for taking representative samples. The cost of sample analysis is reduced due to the analysis of a single sample for a sampling period. In this approach there is always the option of analyzing discrete samples before producing a composite sub – sample.

- Flow – proportional composite sampling

Flow – proportional composite sampling is the process of taking aliquots on a fixed flow volume interval (sampling trigger volume) and instantly mixing the aliquots in a single container to produce a composite sample. There is no opportunity to analyze a single aliquot

in the laboratory or exclude any aliquot. Constituent load is computed using Equation 2.2 and single representative concentration (C_f) is generated from the composite sample.

2.2.3 Turbidity in automated water sampling

Investigating the transport of suspended solids by water sampling usually leads to an underestimation of loads and an unrealistically high sampling frequency is required to properly characterize temporal trends (Littlewood, 1992, Gippel, 1995). The use of surrogate variables which are monitored in situ by sensing devices can provide important information concerning the variable of interest. According to Gippel (1995), field turbidity is an adequate indicator for sediment concentration in most cases. In fact, turbidity peaks during floods usually arrive before flow peaks in an erodible basin, making turbidity a better predictor than water discharge (Thomas, 1985). Thus, turbidity monitored in situ by sensing devices can provide the trigger for sampling to commence (Lewis, 1996).

In 1996 Lewis was one of the first to use turbidity as an auxiliary variable to activate a pumping sampler for the estimation of suspended sediment concentration. According to Lewis, water specimens are pumped during storm events at 10-min intervals. Three pumping samplers holding 24 bottles each are filled in rotation. Lewis followed two study phases. In the first phase, a specified rainfall intensity in combination with a minimum increase in rainfall depth are used to trigger the automatic sampler. Turbidity and SSC are then measured in the laboratory and the extraction of the relation between them, which is found to vary by storm, is possible. In this phase, it was revealed that external relations are unreliable for predicting event loads. In the second phase, using a nephelometric turbidimeter, turbidity is recorded in real time. Sampling begins at the third interval above 20 formazine turbidity units (FTU), at the start of each storm, and stops at the third interval below 20 FTU. The purpose of the system was to cover the range in turbidity and include any major swings. Thus, Lewis established turbidity thresholds for samplings, and specifically different ones were adopted for rising and falling turbidity, as the majority of sediment transport is conducted during the lengthy recession periods. When a certain threshold of rising or falling turbidity is reached, the programmable data logger instructs an automatic pumping sampler to collect a sample. The pumped specimens are analyzed in the laboratory for suspended sediment concentration. The method results in full description of the variation of sediment loads during a flash flood event.

2.3 MODELING

2.3.1 Review of Models for Sediment Transport and Erosion

A wide range of models exists for use in simulating sediment transport and associated pollutant transport. Most erosion models tend to predict erosion for one of the erosion types mentioned in Chapter 2.1.2 or at most a couple. These models differ in terms of complexity, processes considered, and the data required for model calibration and model use. In general there is no ‘best’ model for all applications.

In general, models fall into three main categories, depending on the physical processes simulated by the model, the model algorithms describing these processes and the data dependence of the model:

- Empirical or statistical/metric;
- Conceptual; and
- Physically based.

The distinction between models is not sharp and therefore can be somewhat subjective. They are likely to contain a mix of modules from each of these categories. This classification system used by Wheater et al. (1993) for describing the process representation of the model (empirical, conceptual and physically-based) is adopted in the review of Merritt et al.(2003)

Another enlightening review is given by Papanicolaou et al.(2008). The article aims to trace the developmental stages of current representative 1D, 2D, and 3D models and describe their main applications, strengths, and limitations, providing insight about future trends and needs with respect to hydrodynamic/sediment transport models.

For the purposes of this study, we will refer to models concerning prediction of soil erosion and catchment sediment yield under present and future land use and climate scenarios (de Vente et al, 2013), emphasizing on the objective of each model.

- ART model

Description: The Area Relief Temperature sediment delivery model (ART) (Syvitski et al., 2003, 2005) is a nonlinear regression model which consists of 5 regression equations for 5 climatic zones.

Data requirements: Catchment area (A), large-scale relief (R), and mean annual temperature (T_m)

Objective: It predicts long-term pre-Anthropocene suspended sediment load

- BQART model

Description: a successor of the ART model; it uses 2 global prediction equations (Syvitski and Milliman, 2007).

Data requirements: additional factors include river discharge (Q), lithology, ice cover and human impacts (B) such as dams, land use and erosion control measures.

Objective: BQART predicts long-term average suspended sediment load

- WBMsed

Description: This model integrates BQART with the spatially distributed global daily water balance model WBMplus (Wisser et al., 2010). The model considers each pixel as an outlet of its upstream contributing area and calculates all BQART model parameters on pixel basis (Cohen et al., 2013).

Data requirements: the model needs area, maximum relief, and a lithology factor (static); other parameters are updated during simulations.

Objective: it predicts spatially explicit suspended sediment fluxes. Daily discharge predictions from WBMplus are used to derive long-term average discharge for each pixel.

- Pelletier's model

Description: It is a spatially distributed nonlinear regression model (Pelletier, 2012) that distinguishes detachment of sediment on hillslopes and low order valleys from sediment transport in higher-order alluvial channels. Sediment detachment per soil texture fraction is quantified at a global scale on a pixel basis.

Data requirements: the model requires input data layers for topography, fractions of clay, silt, sand and gravel, mean monthly rainfall and mean monthly LAI (Leaf Area Index)

Objective: It is used to predict suspended sediment yield for pre-dam conditions.

- PSIAC

Description: PSIAC uses nine factors to characterize a drainage basin (PSIAC, 1968). The PSIAC Index (sum of all scores) is then related directly to Suspended Sediment Yield.

Data requirements: the model is based on an expert assessment through field visits, complemented with data on climate, soil, land use, erosion rates and soil conservation practices.

Objective: it predicts the mean annual catchment suspended sediment yield.

- FSM

Description: in the Factorial Scoring Model (FSM), six factors (topography, lithology, vegetation cover, gullies, landslides, and catchment shape) are used to characterize a catchment in the vicinity (~5 km) of its outlet and its main tributaries by providing a score between 1 and 3 for each factor (Verstraeten et al., 2003; de Vente et al., 2005).

Data requirements: the model is based on an expert assessment in the field, complemented with data on the relation between catchment area and suspended sediment yield, data on climate, soil, land use, erosion rates, landslides, and conservation practices

Objective: Assessment of sediment yield

- SPADS

Description: in the SPAtially Distributed Scoring model (SPADS), an index is calculated by multiplying six scores representing vegetation cover, slope, lithology, rainfall intensity, gully density, and the inverse distance from a river stream, using spatially distributed data and predefined decision rules. The average index of a catchment is related to mean annual SSSY through regression (de Vente et al., 2008).

Data requirements: mean monthly rainfall depth or intensity (R factor), Digital Elevation Model (DEM), land use or land cover (C factor), and soil type, texture or soil erodibility estimates.

Objective: Identification of the most important source areas of sediment within the catchment.

- SSSY Index model

Description and Data requirements: four indicators representing processes considered as sources (mass movement and hillslope erosion), sinks (deposits), and transfers of sediments (drainage density) are defined using distributed data. The SSSY Index (sum of indicators) is directly related to mean annual SSSY through regression (Cerdan et al., 2010).

Objective: Identification of dominant erosion processes

- WATEM–SEDEM

Description: The spatially distributed model WATEM–SEDEM consists of three main components: soil erosion assessment, sediment transport capacity calculation, and sediment routing. Soil erosion is predicted with a modified version of the Universal Soil Loss Equation (Renard et al., 1997) for 2 – dimensional landscapes (Van Oost et al., 2000; Van Rompaey et al., 2001; Verstraeten et al., 2002).

Data requirements: Mean monthly rainfall depth or intensity, Digital Elevation Model, land use or land cover, soil type, texture or erodibility, and land management and soil conservation practices.

Objective: it provides estimates of mean annual soil erosion, sediment deposition and sediment yield.

- (Ann)AGNPS

Description: the Annualized AGricultural Non-Point Source Pollution Model (AnnAGNPS) (Bingner and Theurer, 2001) is a physics-based continuous simulation model. Soil erosion and sediment transport are calculated based on the HUSLE equation (Theurer and Clarke, 1991), which uses the RUSLE parameters together with surface runoff and peak rates of surface runoff.

Data requirements: The model requires detailed data on climate, topography, soils, land use, and crops, represented by about 100 parameters for runoff assessments and an additional 80 parameters for SSY prediction.

Objective: The model simulates runoff, erosion, transport of sediments and associated nutrients from hillslopes through channels at a daily timestep.

- LISEM

Description: LISEM (Limburg Soil Erosion Model) is a spatially distributed physics based model simulating runoff and erosion in response to individual rainfall events (de Roo et al., 1996).

Data requirements: The model requires detailed input data on topography, rainfall intensity and duration, LAI, vegetation cover, vegetation height, random roughness, stone cover, soil porosity, initial soil moisture content, soil depth-, cohesion- and texture, aggregate stability, saturated hydraulic conductivity and Manning's n factor.

Objective: Quantification of on – site soil erosion rates

- PESERA

Description: The Pan-European Soil Erosion Risk Assessment (PESERA) model is a physics-based spatially distributed model. Soil erosion is calculated as a function of (1) soil erodibility, based on land use, soil parameters and vegetation cover, (2) the topographic potential, based on a digital elevation model, and (3) the soil erosion potential, based on gridded climate data, vegetation cover, water balance and a plant growth model (Kirkby et al., 2008).

Data requirements: 128 data layers derived from data on climate, topography, land use, crop type, planting date, and soil characteristics, are required to run the model

Objective: prediction of soil erosion by water

2.3.2 The SWAT model

SWAT is a watershed scale, continuous, long-term, distributed model designed to simulate the hydrology, sediment yield and water quality of ungauged watersheds and estimate the impact of land management practices on the hydrology, sediment, and contaminant transport in agricultural watersheds (Arnold et al., 1998). After the subdivision of the watershed into different sub-basins connected by a stream network, SWAT model further divides them into hydrological response units (HRUs). The major model components include hydrology, soil erosion, nutrients, crop growth, and stream routing.

The hydrologic component of each HRU includes the following processes: evapotranspiration, plant uptake, surface runoff and infiltration (using the modified Curve Number or the Green-Ampt method), percolation, lateral subsurface flow, groundwater return flow from the shallow aquifer, deep aquifer losses and channel transmission loss subroutines. Water balance is conducted for the snow compartment, soil, shallow aquifer and deep aquifer. Plant growth is based on the EPIC crop model and uses the "heat units" concept which relates crop growth to the excess of daily temperature above a base temperature. Potential evapotranspiration, leaf area index, rooting depth and soil water content determine the water uptake of plants.

Erosion and sediment yield are estimated for each Hydrologic Response Unit (HRU) with the Modified Universal Soil Loss Equation (MUSLE) (Williams, 1975). The runoff component

of the SWAT model supplies estimates of runoff volume and peak runoff rate, which, with the subbasin area, are used to calculate the runoff erosive energy variable. The current version of SWAT model uses simplified stream power equation of Bagnold's (1977) to route sediment in the channel. Sediment transport in the channel network is a function of two processes, degradation and aggradations (i.e. deposition), operating simultaneously in the reach (Neitsch et al., 2005).

The SWAT system is embedded within a geographic information system (GIS) platform that can integrate various spatial environmental data. The model requires a digital elevation model and input data on land use, land management, soil characteristics, daily rainfall and temperature. Most of the required input parameters (up to 25) are estimated through calibration (Betrie et al., 2011).

3. CASE STUDY

3.1.1 *Koiliaris River Basin*

The area under study is Koiliaris River Basin, situated 15 km east of the city of Chania, in Crete. The basin area is about 130 km², with altitudes between 0 and 2120 m MSL. The springs of Koiliaris River originate from the White Mountains and the total length of the river is 36 km. Koiliaris is joined with four tributaries, from which two are temporary rivers (Keramianos and Anavreti) and two are permanent ones.

Geologically, the area is characterized by the limestone – karstic system in the south part which lies beneath impermeable deposits of marls and schists in the northern part, which also includes alluvial deposits. The springs of Koiliaris River are: Stilos, Anabreti, Vlixada, Koliakon (about 170 * 10⁶ m³/year). The springs of Armenon and Stilos have large seasonal fluctuations of their flow and have mean annual flow: 769 l/s and 2654 l/s respectively. The spring of Kalives (Zourbos) has similar mean annual flow 978 l/s and small seasonal fluctuation. The quality of water that is supplied by the White Mountains is excellent.

The total flow at the exit point of the basin outlet was estimated to be 136.29 million m³/year. From this, 80% was contributed by the karstic flow through Stilos springs, while the net contribution of watershed flow (Keramiotis and Anavreti tributaries) to the river was only 20% of the total flow (Kourgialas et al., 2010). The river hydrograph is characterized by peaks of quick and slow response. The quick response was mainly due to surface runoff and the slow response due to springs flow recession (Moraetis et al., 2010). The river hydrograph is characterized by a series of flash floods peaks. These sharp peaks are mainly attributed to Keramianos tributary during the rainy season (Kourgialas et al., 2010; Moraitis et al., 2010). The flood wave is generated in the upstream non-karst watershed and travels to the karstic area.

As far as the land uses are concerned, rangeland accounts for 58% (101 km²) of the total watershed area. Cultivated areas cover 29,4% (51km²), urban 2,8% (5 km²), forests 8,5% (14,8 km²), and aquatic areas 0,6% (1km²). The watersheds in not industrialized and most of the people work in agriculture (the main cultivated species are olive trees, orange trees and vines). Koiliaris River crosses the plain (154.500 acres) of the Municipality of Apokorona where there is abundance of natural ecosystems. At the foot of White Mountains there are forests with firs and bushy areas with various species of bushes and flowers. It includes also various species of trees as fig trees, platans and a large area with olive trees.

There are three (one telemetric) hydrometric stations and three (two telemetric) meteorological stations inside the basin, as shown in Figure 3.1, while there are two hydrometric stations outside the basin, one in the extended karstic area. Data at each station are recorded every 5 minutes. Hydrometric station H3 reports the hydrological data of the upstream non-karst watershed, and station H2 the data of the downstream karstic area (Figure 3.1). During the last 30 years, many extreme flash flood events have occurred in the basin, especially in the downstream area (Hydrometric station H1).

The main type of soil degradation in the basin is water erosion, which is due to the clearing of forests and natural vegetation for cropping and livestock grazing. De-vegetation and inappropriate cultivation practices induces soil organic matter losses making soils susceptible to erosion and desertification with global consequences for food security, climate change, biodiversity, water quality, and agricultural economy.

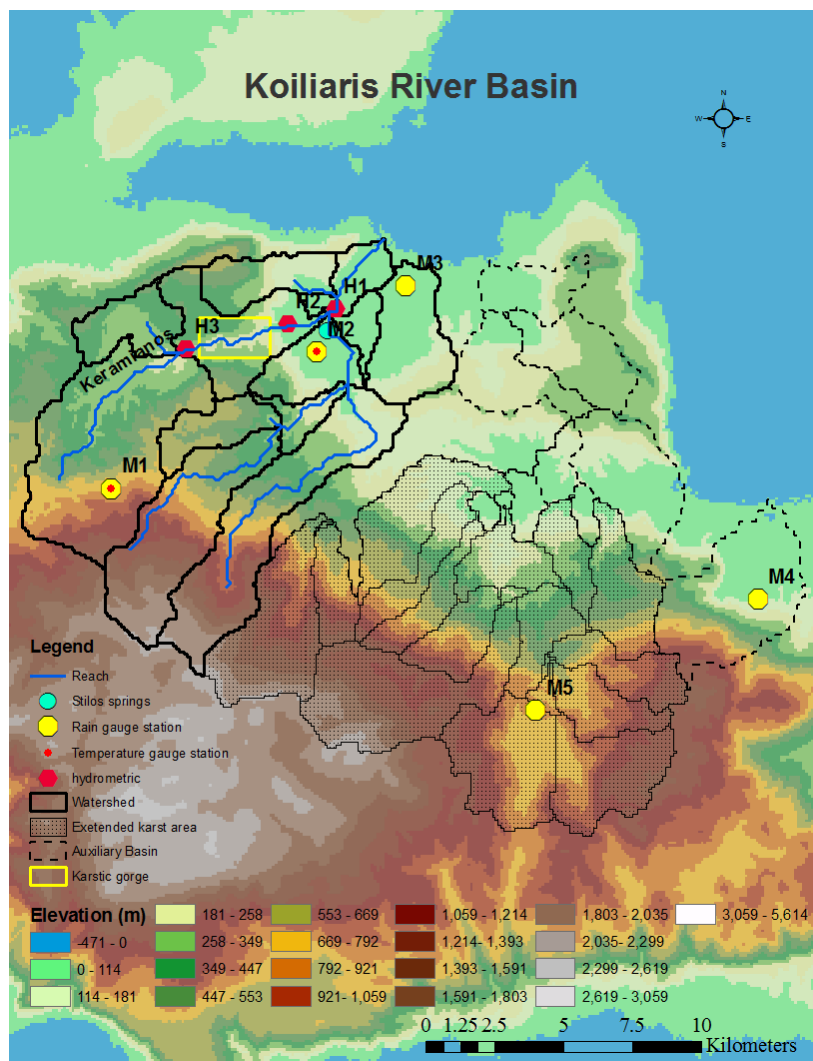


Figure 3.1: Koiliaris River (extended) Basin and hydrometeorological network.

3.1.2 Peculiarity of Koiliaris Watershed

Karst systems in the Mediterranean region have the special feature that a spring could receive contributions from the karst that is extended outside the watershed boundaries to which the spring belongs or karst situated one on top of another with different hydraulic characteristics and thus different transmissivities (Nikolaidis et al., 2013). This fact underlies the importance of the identification of the extended karst area that contributes to the flow of a spring for the acquisition of accurate hydrologic and geochemical balances of the system (Tzoraki and Nikolaidis, 2007; Moraetis et al., 2010). In our case, the karst system is characterized by fast infiltration and direct connection to the conduits below. There are two main series of springs in which the karst system discharges: Stilos springs at elevation +17 m a.m.s.l. and an intermittent spring, Anavreti at +24 m a.m.s.l. Both of them feed Koiliaris River. The total recharge area of the springs extends beyond the boundaries of Koiliaris River Basin to the southeast of the watershed boundary. The geology of the region in combination with a major fault in a northeast – southwest direction directs the water towards the springs in the Koiliaris River Basin (Moraetis et al., 2010; Nikolaidis et al., 2013).

3.1.3 Sediment transport in the Koiliaris River

The sampling point for suspended sediment is located just downstream of the cross-section, where the Keramianos tributary merges with the main river, the latter being fed by the karst springs. The Keramianos tributary drains a small sub-catchment that generates surface runoff due to a schist geologic formation before entering a karstic gorge (Figure 3.2). Schist alone is quite friable (Asseline et al., 1994) and in combination with the steep slopes and the agricultural and rural practices that are exerted in the area, the top soil becomes extremely brittle and easily transported. Specifically, due to changes in agricultural practices over the years, tractors now enter and plough the terraces, leading to their failure and exacerbating the erodibility of the ground. In addition, overgrazing leaves the top soil unprotected and vulnerable to surface runoff.

Thus, Keramianos is the main tributary responsible for the sediment transport in Koiliaris River. The other tributary of Koiliaris, the one derived from the karst springs, has a relatively constant - low - concentration (equal to 4 mg/l) (Figure 3.4a). However, only two to four times a year, during flood conditions when daily precipitation in meteorological station M1 exceeds 120mm, Keramianos tributary actually merges with Stilos Springs, transferring

significant loads of suspended sediment; for precipitation lower than this threshold, Keramianos disappears in the karstic gorge. In Figure 3.3 the mixing of the two flows of different sediment concentrations at Ag. Georgios station (H1) is illustrated.

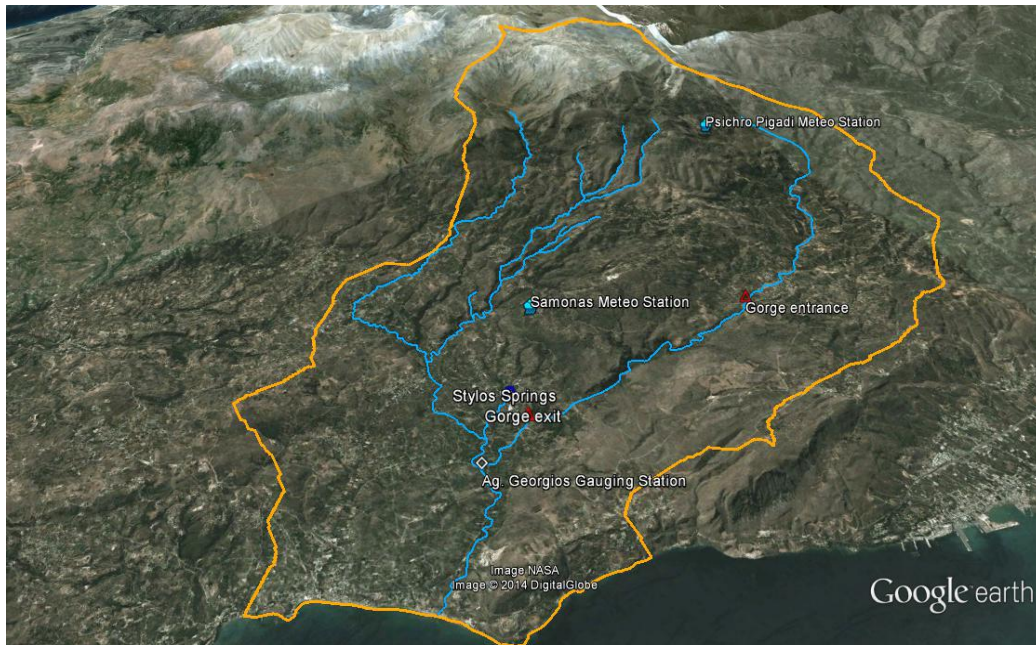


Figure 3.2: Koiliaris River Watershed



Figure 3.3: Mixing of two flows: Stylos Springs with low sediment concentration (left) Keramianos tributary with high sediment concentration (right).

Due to the fact that Keramianos reaches the tributary coming from the springs only twice or four times a year, we conducted the study of sediment transport upstream, at Keramianos tributary (Figure 3.4b), where the suspended sediment concentration is abundant after intense rainfall. In order to ensure that the conditions concerning suspended sediment are the same upstream and downstream of the gorge, we performed a grain size analysis for samples of both locations. The grain size analysis was combined with an XRF analysis to obtain a comprehensive view of the suspended sediment in the watershed.



Figure 3.4: a) Ag. Georgios station b) Keramianos river and data logger.

4. METHODOLOGY

4.1 INTRODUCTION

The study of sediment transport, conducted for the Koiliaris river, can be divided into three major sections: Sampling and monitoring, analysis of samples, and modeling.

As far as sampling is concerned, the estimation of river suspended sediment is carried out mainly by laboratory filtration of grab water samples. This technique provides only a rough estimation of the sediment transport. To overcome this, as well as to have the ability to collect representative sediment transport data during extreme flow events (e.g. flash floods), an automated sediment sampling device (Sediment Trap) is developed and described herein. The testing of the device could not be performed at the station of Ag. Georgios, where the system will be deployed, due to the fact that only once or twice a year high loads of sediment appear at that point and the fact that the past year was a dry year. Therefore, we tested the device at the Keramianos river, upstream, after examining if the sediment there has approximately the same size distribution with the sediment at Koiliaris river (Ag. Georgios station).

The analysis of samples includes estimation of suspended sediment concentration by both Standard Gravimetric Analysis and Spectrophotometric Analysis. X-Ray Fluorescence (XRF) analysis was carried out to determine the chemical characterization of samples for a comprehensive understanding of the sediments and the grain size distribution was determined by a laser diffraction particle size analyzer. An additional purpose of the latter was to examine whether sediment collected from Keramianos has the same particle size distribution with sediment collected from Ag. Georgios. Furthermore, field measurements of turbidity were correlated with suspended solids concentrations derived from grab sampling, and an empirical curve between turbidity and suspended sediment concentration was developed.

Modeling of suspended sediment concentration was conducted through the Sediment Component of the SWAT model, after the hydrology of the basin was simulated (Nikolaidis et al., 2013). We used a modified version of the SWAT model proposed by Nikolaidis et al. (2013) which takes the contribution of the extended karst area into account.

4.2 SAMPLING AND MONITORING

4.2.1 Grab Sampling

Grab samples from Ag. Georgios hydrometric station (H1), were taken on a monthly basis from 2011 to 2014. Water samples of 2 l volume were filtered through pre-weighted filters of 2 – 3 micron porosity. The suspended sediment of each sample was determined by the filter's weight increment after drying it (Standard Gravimetric Analysis). For comparison purposes, the DR 2800 Spectrophotometer was also used. This method directly determines total suspended solids in a sample with a measurement wavelength of 810 nm. Measurements exported from the spectrophotometer were close to the ones estimated by the filtration method ($r^2 = 0.95$).

As shown in Figure 4.1, through the standard procedure of grab sampling only low concentrations of suspended sediment were recorded, with the exception of the sample taken on 4/12/2013. These continuous low concentrations correspond to the clear waters originating from the karstic springs and have a mean concentration of 4 mg/l. On the 15/11/2013, during the first intense rainfall of the hydrologic year, the Suspended Sediment Concentration (SSC) at Ag. Georgios station was 12 mg/l, stating instantaneous sediment transport due to surface runoff. However, on the 4/12/2013, when daily rainfall at meteorological station M1 was 123.2 mm, Keramianos exited the karstic gorge and joined with the permanent flow of the karstic springs, transferring significant amounts of sediment. The two flows of different sediment concentration were mixed at the point of the station, with a common concentration of about 300 mg/l (Figure 4.1).

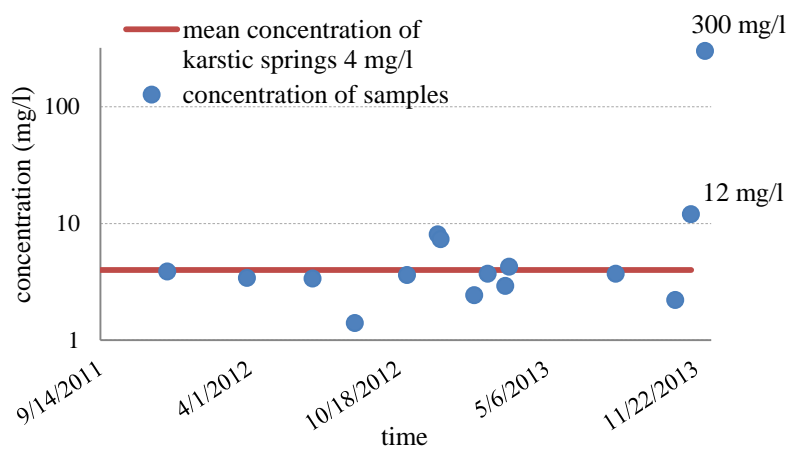


Figure 4.1: Suspended Sediment Concentration at Ag. Georgios station

The fact that we did not acquire the desired amount of samples which would contain sediments produced by flash floods, is due to the infrequency of intense rainfall, a characteristic of the Mediterranean region, as well as due to the difficulty of conducting measurements during extreme conditions.

4.2.2 Limitations from Grab Sampling and suggested method

As mentioned in the previous section, adverse field conditions do not allow for sediment measurements (using grab samples) to be conducted during periods of high sediment concentrations, such as flash floods, or first flash events in temporary rivers, when most of the annual suspended sediment is usually transported. Automatic measuring of suspended sediment concentration (SSC) is thus preferable over grab sampling or other methods of manual collection of suspended sediment, but the high frequency sampling, necessary during extreme events, is expensive and impractical if performed continuously. Thus, an ideal method would be the continuous measuring of water discharge and the occasional discrete sampling of water specimens for suspended sediment concentration analysis.

In our case, the system works as follows: when a certain threshold of rising or falling turbidity is reached, the programmable data logger instructs an automatic pumping sampler to collect a sample. The pumped specimens are analyzed in the laboratory for suspended sediment concentration. The method results in full description of the variation of sediment loads during a flash flood event.

The proposed automatic sediment sampling system is being implemented at Ag. Georgios River Gauging Station, where the Hydrometric station H1 is installed. As mentioned earlier, the gauging station H1 was located just downstream of the merge of the two flows; the permanent one from Stilos springs and the temporary one from Keramianos tributary. The channel at this point is about 8.5 m wide with an average depth of 0.70 m.

4.2.3 System Architecture

Flow-weighted or volume-paced method uses a flowmeter and automated sampler. When a specified volume has passed the monitoring point, the flowmeter triggers the automated sampler to draw a small volume (50ml-500ml) of sample. These are known as aliquots (See Chapter 2.2.2). The sampler will continue to draw aliquots at the specified intervals.

Therefore, at higher flow rates, the aliquots are taken more frequently and the composite of all these aliquots is the flow-weighted composite sample; the sample is “weighted” towards the higher flow rates. The analytical result for this single sample is equivalent to an Event Mean Concentration (EMC) for the storm (Lopes et al., 2000). Constituent load is computed using the Equation 2.2 and single representative concentration \bar{c} , is generated from the composite sample.

The innovation of the presented system is the fact that there is no limitation on the volume of water sampled, as the composite sample passes through the filter and only the suspended sediment is retained. Another difference with usual flow proportional water sampling techniques is that, now, what changes in proportion to the flow is the pumping rate, and not the density of the samples.

Specifically the system operates as described by Sibetheros et al. (2013): The expected maximum peak flow from the watershed of Koiliaris, according to historical data is 80 m³/s and the interval between 20 and 80 m³/s is divided into 6 volumetrically equal classes of 10 m³/s each. We also divide the rate of pumping into 6 classes. The pumping rate is automatically augmented a class, every time the flow surpasses a class. Water stage is monitored every five minutes and it is converted to flow by the rating curve for the specific site conditions. Thus, water specimens are pumped during storm events and the pump rotation is proportional to the stage, allowing for a flow weighted sampling. Water is pumped from an intake nozzle which is designed to be positioned at 60% of the flow depth for a representative sample (Lecce, 2009). Sampling is initiated automatically when at least one of the two conditions holds:

- *Water surpasses a certain level:* The system’s onboard controller initiates river stage data collection from the level sensor (with increased rate) and converts them to flow. This is possible with the utilization of a rating curve for the specific site (water level to discharge relationship). Based on flow measurements conducted from 2004 to 2014, a two-part rating curve has been defined: When the water level H at hydrometric station is lower or equal to 0.5 m then the flow discharge is computed using the equation:

$$Q = 0.35H \left(m^3 / s \right) \quad (4.1)$$

When the water level H at H1 is over the 0.5 m, then the flow discharge is given by

$$Q = 36.33H - 17.3 \left(m^3 / s \right) \quad (4.2)$$

The rating curve is being continuously updated. If water stage surpasses 1.0 m, meaning that flow surpasses 20 m³/s, the sampling initiates.

- *Turbidity surpasses a certain threshold* (thus signaling a flood event): Turbidity is constantly recorded at the station by the turbidity sensor of the Multi-Parameter Water quality TROLL 9500 (In-Situ Inc.). An appropriate turbidity threshold for our case is considered 30 NTUs, so that the contribution of the Keramianos tributary will be taken into account, and “false alarms” because of instantaneous sediment transport from surface runoff will not exist.

The water sample then passes through a sediment trap (5μm filter, see also Chapter 5.2.1) that captures the sediment. The solids are weighted once a week or after each storm and the data are converted into the total suspended sediment flux as follows: If M_{filter} is the suspended sediment mass captured by the filter and q_{pump} is the pump rate, the total sediment mass during a flood can be estimated by

$$M_{total} = M_{filter} \cdot \frac{\sum V}{\int q_{pump} dt} \quad (4.3)$$

where $\sum V$ is the total water volume during a flood event, as estimated by the stage at each interval. We can then have a rough estimate of the mean suspended sediment concentration during the flood event:

$$\bar{s} = \frac{M_{total}}{\sum (Q\Delta t)} \quad (4.4)$$

The automatic sampling system is currently undergoing testing to ensure it can function under severe conditions.

Figure 4.2a depicts the setup of the system: water stage and turbidity sensors signal for the event, and the pump initiates the rotation, on a rate which depends on the signal. Then, water passes through the sediment trap, where it is filtered. Figure 4.2b shows the actual battery – operated device; the electronic system and the battery are inside the trap, whereas the pump and filter are on the side. In Figure 4.3, the behavior of turbidity and water stage during river rising is depicted. In this case turbidity and water level surpassed the above mentioned thresholds almost simultaneously; however, even though turbidity was zeroed three hours after the initiation of the phenomenon, water stage was over 1.0 m even 11 hours later. In our

case, sampling will be continued until water stage falls under 1.0 m in order to have a complete overview of the phenomenon.

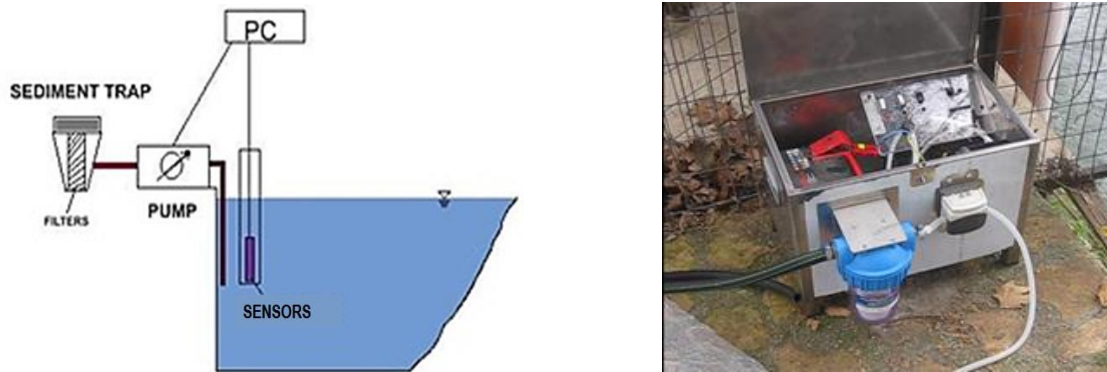


Figure 4.2: (a) Sediment trap setup (b) Sediment trap prototype

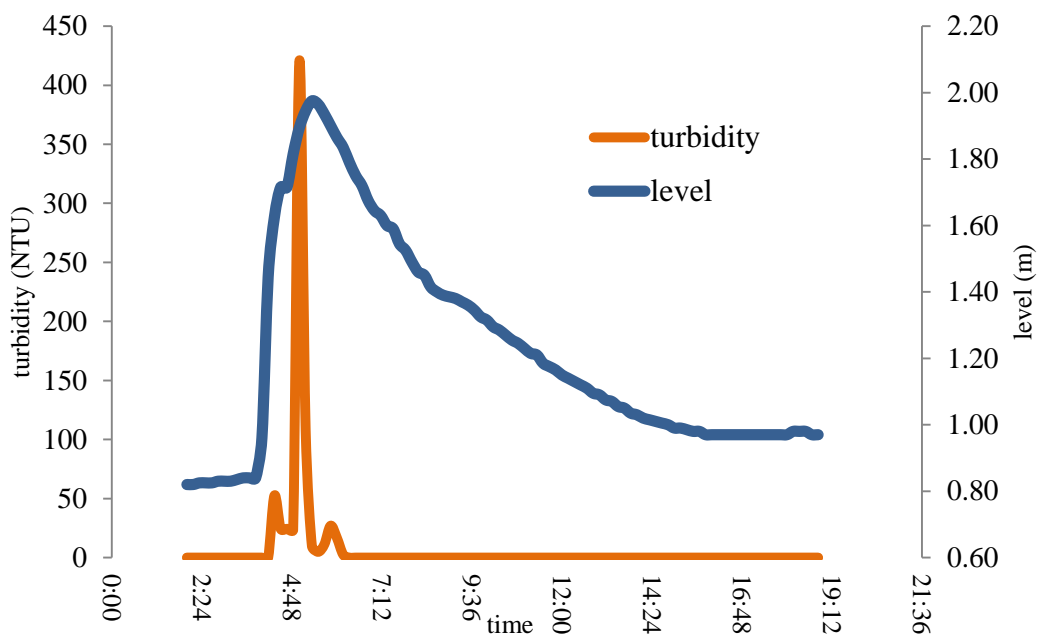


Figure 4.3: Water level and turbidity during river rising at Ag. Georgios (on 23/12/2012)

4.3 SUSPENDED SEDIMENT ANALYSIS

4.3.1 Grain Size Analysis

Grain size analysis was carried out in order to compare samples taken from different periods and locations. The sediment was very fine, thus laser diffraction was used; it is a widely used technique for particle size characterization of materials with a grain diameter ranging from hundreds of nanometers up to several millimeters. Laser diffraction measures particle size distributions by measuring the angular variation in intensity of light scattered as a laser beam passes through a dispersed particulate sample.

A conventional analysis (Folk, 1966) of four samples taken from Keramianos on 15/11/2013, 4/12/2013 and 2/1/2014 and from Ag. Georgios on 4/12/2013 was initially made. The phi unit was used; it is a logarithmic transformation of millimeters into whole integers, according to the formula:

$$\Phi = -\log_2 d \quad (4.6)$$

where d is the grain diameter (mm).

For the conventional analysis, the following statistical tools were calculated:

- Mode: the most frequent size category – the largest column of the histogram.
- Graphic Median: 50% of the observations are above and 50% below this category. The phi value at 50% is the Median of the sample or grain population.
- Graphic Mean: the average size category. It is given from:

$$M = \frac{\phi_{16} + \phi_{50} + \phi_{84}}{3} \quad (4.7)$$

The characterization of the sample, according to the Mean is given from Table 4.1

Table 4.1: Grain Size

Characterization	Phi units
Boulder	-12 to -8 phi
Cobble	-8 to -6 phi
Pebble	-6 to -2 phi
Granular	-2 to -1 phi
Very coarse grained	-1 to 0 phi
Coarse grained	0 to 1 phi
Medium Grained	1 to 2 phi
Fine grained	2 to 3 phi
Very fine grained	3 to 4 phi
Coarse silt	4 to 5 phi
Medium silt	5 to 6 phi
Fine silt	6 to 7 phi
Very fine silt	7 to 8 phi
Clay	8 phi and smaller

- Inclusive Graphic Standard Deviation: a measure of sorting or variation in sizes

$$D = \frac{\phi_{16} + \phi_{50} + \phi_{84}}{3} \quad (4.8)$$

Depending on the value of the standard deviation, we can draw conclusion about the degree of sorting of the sample (Table 4.2)

Table 4.2: Sorting

Characterization	Phi units
Very well sorted	Under 0.35 phi
Well sorted	0.35 to 0.50 phi
Moderately well sorted	0.50 to 0.71 phi
Moderately sorted	0.71 to 1.00 phi
Poorly sorted	1.00 to 2.00 phi
Very poorly sorted	2.00 to 4.00 phi
Extremely poorly sorted	over 4.00 phi

- Inclusive Graphic Skewness: shows if the distribution is bell shaped or shifted to the side

$$S = \frac{\phi_{84} + \phi_{16} - 2\phi_{50}}{2(\phi_{84} - \phi_{16})} + \frac{\phi_{95} + \phi_5 - 2\phi_{50}}{2(\phi_{95} - \phi_5)} \quad (4.9)$$

The characterization of the skewness is presented in Table 4.3

Table 4.3: Sorting skewness

Characterization	Phi units
Very fine – skewed	1.0 to 0.3 phi
Fine – skewed	0.3 to 0.1 phi
Near symmetrical	0.1 to - 0.1 phi
Coarse – skewed	- 0.1 to - 0.3 phi
Strongly coarse – skewed	- 0.3 to - 1.0phi

- Kurtosis: shows if the distribution is bell shaped, very flat, or very peaked

$$K = \frac{\phi_{95} - \phi_5}{2.44(\phi_{75} - \phi_{25})} \quad (4.10)$$

The characterization of the kurtosis is presented in Table 4.4

Table 4.4: Sorting kurtosis

Characterization	Kurtosis
Very platykurtic	< 0.67
Platykurtic	0.67 to 0.90
Mesokurtic	0.90 to 1.11
Leptokurtic	1.11 to 1.50
Very leptokurtic	1.50 to 3.00
Extremely leptokurtic	> 3.00

In an attempt to test whether or not samples from Keramianos change over time and whether the samples taken from Keramianos are the same with the ones selected from Ag. Georgios, tests of significant differences were conducted.

The grain-size distributions obtained in this study are statistically independent of each other and described by only one variable (grain size). Statistical tests are usually used to find a significant difference within sampled data sets (Henkel and Ramon, 1976). However, a statistical problem exists when comparing grain-size distributions. Since a grain-size distribution is expressed in terms of weight percentage, the number of samples (n) for a grain-size distribution cannot be defined. Therefore, we considered $n = 100$ as proposed by Kurashige and Fusejima (1997) as a sample size with sufficient power to detect a significant difference in grain-size distributions.

Since the normality test (Anderson – Darling) showed that the samples did not follow the normal distribution (Folk and Ward, 1957; Inokuchi and Mezaki, 1974), the non – parametric

Mann-Whitney – U test was applied. The null hypothesis is that the distributions of every pair of groups are identical, so that there is a 50% probability that the value of a randomly selected observation one of a population, exceeds an observation randomly selected from the other population.

The test involves the calculation of a statistic, usually called U , whose distribution under the null hypothesis is known. Both groups of data are taken together, and ranked; rank 1 is given to the lowest score etc. Tied ranks are given the average of the tied ranks. The sum of the ranks (T) are found for each sample. The value U is calculated for each sample:

$$U = (N_1 \cdot N_2) + \left(\frac{N_1 \cdot (N_1 + 1)}{2} \right) - T_1 \quad (4.11)$$

As N_1 and N_2 increase in size, the sampling distribution of U rapidly approaches the normal distribution, with

$$mean = \mu_u = \frac{N_1 N_2}{2} \quad (4.12)$$

$$stdev = \sigma_u = \frac{N_1 N_2 (N_1 + N_2 + 1)}{12} \quad (4.13)$$

Thus when $N_2 > 20$, the significance of an observed value of U is determined by:

$$z = \frac{U - \mu_u}{\sigma_u} \quad (4.14)$$

which is practically normally distributed with zero mean and unit variance, i.e., the probability associated with the occurrence under H_0 values as extreme as an observed z may be determined by reference to tables of z . If a one-tailed test is being used, then the observed z is significant at $p = 0.05$ if it is $z > 1.64$.

Finally, in order for the mean values of the samples that were taken from different locations to be compared, an approach similar to the one of Gardner (1993) was used. Each $\Phi 50$ value was considered as a sample and the average $\Phi 50$ of the samples collected from Keramianos, were compared with the ones from Ag Georgios using the analysis of variance (ANOVA).

4.3.2 Geochemical Analysis

X-ray fluorescence (XRF) spectrometry is a widely-used technique for the routine determination of the major elements as well as a large number of geochemically important

trace elements in geological samples. It is often the preferred technique for determining the major elements in rocks (Na, Mg, Al, Si, P, K, Ca, Ti, Mn, Fe), where uncertainties less than 0.2 to 0.4% relative are required to ensure confident summation of major elements to 100% (Potts et al., 1992).

X-Ray Fluorescence is defined as “The emission of characteristic “secondary” (or fluorescent) X-rays from a material that has been excited by bombarding with high-energy X-rays or gamma rays. The phenomenon is widely used for elemental analysis. When high energy photons (x-rays or gamma-rays) are absorbed by atoms, inner shell electrons are ejected from the atom, becoming “photoelectrons”. This leaves the atom in an excited state, with a vacancy in the inner shell. Outer shell electrons then fall into the vacancy, emitting photons with energy equal to the energy difference between the two states. Since each element has a unique set of energy levels, each element emits a pattern of X-rays characteristic of the element, termed “characteristic X – rays”. The intensity of the X-rays increases with the concentration of the corresponding element.

For the determination of the above elements in suspended sediment, due to the fact that only quantities of maximum 2 gr of dry mass were available, glass discs were used (Alvarez, 1990). The sediment samples had been burnt at 1050 °C before the analysis. Three samples from Keramianos taken on three different dates were analyzed, in order to test the variation of the samples over time.

4.3.3 Turbidity – suspended sediment concentration curve

Research conducted by the Pacific Southwest Research Station of the U.S. Forest Service showed that simple linear regression of turbidity and sediment samples provided a more accurate daily prediction of sediment loads than discharge-derived methods (Lewis, 1996). In this study, field measurements of turbidity were correlated with suspended solids concentrations derived from grab sampling, and an empirical curve between turbidity and suspended sediment concentration was developed. In this way, the establishment of the starting conditions of the device and the awareness of the suspended sediment concentration of the river at any time, just by reading the turbidity signal, is possible.

In order to establish this relation, field visits at Keramianos and Koiliaris under different precipitation and flow conditions (which means different sediment transport conditions) were performed. Turbidity at a specific point of the river was measured at different time instants

with the turbidity sensor, and samples were taken from that exact point. The samples were later analyzed in the laboratory and SSC was measured using both the standard filtration method and the spectrophotometer.

4.4 MODELING

4.4.1 Augmented SWAT Model

Due to the peculiarity of the Koiliaris watershed, an augmented version of the SWAT model, proposed by Nikolaidis et al. (2013) was used, in order to simulate the contribution of the extended karst to the spring discharge and account for the variability of the discharge recession due to two karst formations. The precipitation in the karstic area of the watershed is directed to deep groundwater after SWAT simulates surface hydrologic processes such as snow accumulation and melt, surface runoff, infiltration to shallow groundwater and evapotranspiration. The deep groundwater flow from SWAT in the karstic area that could be related to a specific spring is aggregated on a daily basis and becomes the input flow to a two-part reservoir karst model.

A brief description of the modified karst model follows (Fig. 4.3). The major modification from the previous versions is that the input flow is the deep groundwater flow from SWAT. The hydrologic mass balances of the karst model are:

Upper reservoir mass balance:

$$\frac{dV_1}{dt} = Q_{in,1} - Q_1 \quad (4.15)$$

Lower reservoir mass balance:

$$\frac{dV_2}{dt} = Q_{in,2} - Q_2 \quad (4.16)$$

Where:

$$Q_{in,1} = a_1 \cdot Q_{in,deepGW} \quad (4.17)$$

$$Q_{in,2} = (1 - a_1) \cdot Q_{in,deepGW} + a_2 \cdot Q_1 \quad (4.18)$$

$$Q_1 = K_u \cdot V_1 \quad (4.19)$$

$$Q_2 = K_l \cdot V_2 \quad (4.20)$$

and $Q_{in,deepGW}$ is the deep groundwater flow from SWAT, a_1 is the fraction of karst with the upper reservoir, a_2 is the fraction of flow from the upper reservoir discharge entering the

lower reservoir and K_u and K_l are recession constants (1/d) for the upper and lower reservoir. For constant $Q_{in,1}$ and $Q_{in,2}$ (daily time step) the analytical solutions of (4.7) and (4.8) follow:

$$Q_1 = Q_{1,0}e^{-K_u t} + Q_{in,1}(1 - e^{-aK_u t}) \quad (4.21)$$

$$Q_2 = Q_{2,0}e^{-K_l(1-a_2)t} + (1-a_1)Q_{in,2}(1 - e^{-K_l(1-a_2)t}) \quad (4.22)$$

The total karstic flow is then calculated:

$$Q_{karstic} = (1-a_2)Q_1 + Q_2 \quad (4.23)$$

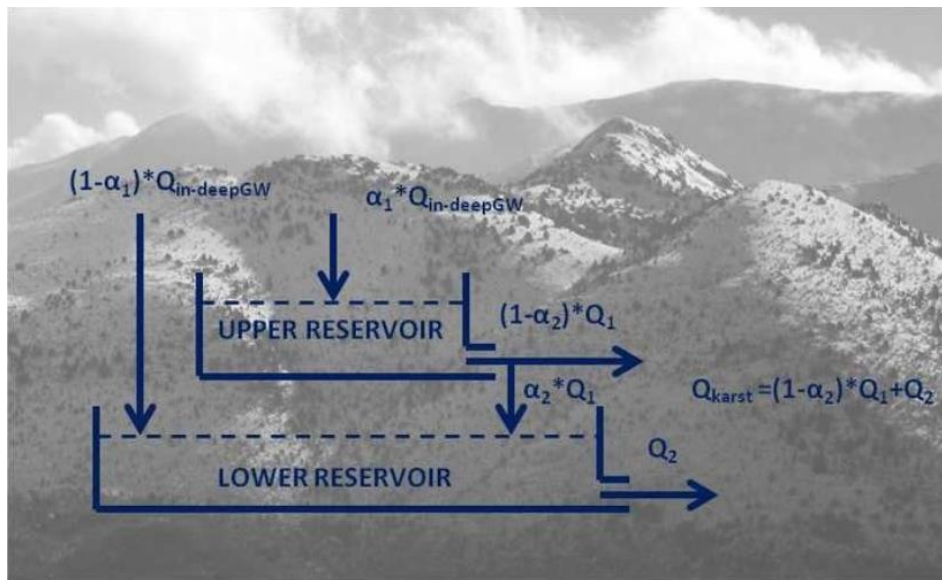


Figure 4.3: Conceptual schematic of the karst model (Nikolaidis et al., 2013).

The model has already been calibrated for the Koiliaris watershed until 2010 (Nikolaidis et al., 2013), and for the present study it was set to simulate four more years (2010-2014), for which daily flow data are available.

4.4.2 Model Input and Data Processing

Mandatory GIS input files needed for the SWAT model include the Digital Elevation Model (DEM), land cover, and soil layers. After importing these files, and defining the main slope classes of the watershed, the HRUs – which are unique combinations of a land use, a soil type and a slope - are defined. Weather data from stations within the region were incorporated to provide the most representative precipitation and temperature data available. Other

meteorological data required by SWAT (solar radiation, wind speed, and relative humidity) are estimated using the SWAT weather generator.

Weather data for the watershed were available from two meteorological stations (Samonas and Psichro Pigadi stations – stations M2 and M1 respectively) operated by the Technical University of Crete as well as from other three meteorological stations (Askyfou, Mouri and Kalyves stations for precipitation data only – stations M3 to M5) operated by the Borough of Crete. Precipitation and temperature at Samonas and Psichro Pigadi are monitored every five minutes and aggregated on a daily level so that they can be imported in the SWAT Model. Precipitation data from the other three meteorological stations are available on a daily step. Missing data from a station were completed using rainfall gradient or correlation between stations.

Specifically, data from meteorological stations M3-M5 correspond to the 1973-2009 time period and since 2007, when installed, the meteorological stations M1 and M2 record rainfall and temperature every five minutes allowing for a high frequency monitoring. Stations M1 and M2 are located at 1000 and 385 m a.m.s.l. respectively. The hydrometric station H1, installed in 2004, is located just downstream of the intersection of the tributary and the main river; Prior to the installation of the hydrometric station, monthly flow data were available since 1973. For the verification of discharge simulation by SWAT (Refsgaard, 1997), stage data from the station H1 were transformed into discharge through an equation (rating curve) developed for the specific cross-section, using flow and stage measurements conducted during the 2005-2013 period (See Chapter 4.2.3).

As far as the suspended sediments are concerned, grab samples from Ag. Georgios hydrometric station (H1), taken on a monthly basis from 2011 to 2013, were used to calibrate the sediment concentration simulations. For a further evaluation of the sediment concentration output of the model, from December 2013 to February 2014, grab samples were also taken from the Keramianos tributary (hydrometric station H3). Water samples were filtered using pre-weighted filters, then the filters were let to dry out; the increase of each filter's weight corresponded to the suspended sediments' weight in each grab sample.

4.4.3 Sediment Equations

Erosion caused by rainfall and runoff is computed with the Modified Universal Soil Loss Equation (MUSLE) (Williams, 1975). MUSLE is a modified version of the Universal Soil Loss Equation (USLE) developed by Wischmeier and Smith (1978)

USLE predicts average annual gross erosion as a function of rainfall energy. In MUSLE, the rainfall energy factor is replaced with a runoff factor. This improves the sediment yield prediction, eliminates the need for delivery ratios, and allows the equation to be applied to individual storm events. Sediment yield prediction is improved because runoff is a function of antecedent moisture condition as well as rainfall energy. Delivery ratios (the sediment yield at any point along the channel divided by the source erosion above that point) are required by the USLE because the rainfall factor represents energy used in detachment only. Delivery ratios are not needed with MUSLE because the runoff factor represents energy used in detaching and transporting sediment.

The modified universal soil loss equation (Williams, 1975) is:

$$S = 11.8 \cdot (Q \cdot q \cdot A)^{0.56} \cdot K \cdot C \cdot P \cdot LS \cdot F \quad (4.24)$$

where S is the sheet erosion on a given day (metric tons), Q is the surface runoff volume (mm water), q is the peak runoff rate (m^3/s), A is the area of the HRU (ha), K is the USLE soil erodibility factor, C is the USLE cover and management factor, P is the USLE support practice factor, LS is the USLE topographic factor, and F is the coarse fragment factor.

Sediment deposition and channel degradation are the two dominant channel processes that affect sediment yield at the outlet of the watershed. Sediment transport consists of two components 1) Landscape component and 2) Channel component. From the landscape component, SWAT keeps tracks of the particle size distribution of eroded sediments and routes them through ponds, channels and surface water bodies. In the channel, degradation or deposition of sediment can occur depending on the stream power, the exposure of channel sides and bottom to the erosive force of the stream and the composition of channel bank and bed sediment. Whether channel deposition or channel degradation occurs depends on the sediment loads from upland areas and transport capacity of the channel network. If sediment load is larger than its sediment transport capacity, channel deposition will be the dominant process. Otherwise, channel degradation occurs over the channel segment. SWAT estimates

the transport capacity of a channel segment as a function of the peak channel velocity (Equation 4.25):

$$T_{ch} = a \times v^b \quad (4.25)$$

Where T_{ch} (ton m⁻³) is the maximum concentration of the sediment that can be transported by streamflow (i.e., transport capacity), a and b are user defined coefficients and v (m/s) is the peak channel velocity. The peak velocity in a reach segment at each time step is calculated from

$$v = \frac{a}{n} \times R_{ch}^{2/3} \times S_{ch}^{1/2} \quad (4.26)$$

Where a is the peak rate adjustment factor with a default value of unity, n is Manning's roughness coefficient, R_{ch} is the hydraulic radius (m) and S_{ch} is the channel invert slope (m/m). Channel degradation (S_{deg}) and deposition (S_{dep}) in tons are computed as:

$$S_{dep} = \begin{cases} (S_i - T_{ch}) \times V_{ch} & ; S_i > T_{ch} \\ 0 & ; S_i \leq T_{ch} \end{cases} \quad (4.27)$$

$$S_{deg} = \begin{cases} (T_{ch} - S_i) \times V_{ch} \times K_{ch} \times C_{ch} & ; S_i < T_{ch} \\ 0 & ; S_i \geq T_{ch} \end{cases} \quad (4.28)$$

Where S_i is the initial sediment concentration in the channel segment (ton/m³), V_{ch} is the volume of water in the channel segment (m³), K_{ch} is the channel erodibility factor (cm/h/Pa), and C_{ch} is the channel cover factor. The amount of sediment that is transported out of the channel segment (S_{out}) in tons is computed as:

$$S_{out} = (S_i + S_{deg} - S_{dep}) \times \frac{V_{out}}{V_{ch}} \quad (4.29)$$

where V_{out} is the volume of water leaving the channel segment (m³) at each time step.

4.4.4 Erosion Parameters

Calibration for suspended sediment was conducted with the following logic: erosion parameters were altered for the subbasin of Keramianos in such a way so that the soil depletion of the area could be expressed and extreme events of sediment transport at Ag. Georgios station due to the tributary of Keramianos could be depicted.

- Soil erodibility factor

Soil erodibility is a term used to describe the difference in the degree in which different soils erode when all other factors are the same. Soil erodibility is caused by the properties of the soil itself. It has been observed that a soil type usually becomes less erodible with decrease in silt fraction, regardless of whether the corresponding increase is in the sand fraction or clay fraction. The soil erodibility factor ranges in values from 0.02 to 0.69 (Goldman et al. 1986). Stewart et al. (1975) also developed a table indicating the general magnitude of the *K*-factor as a function of organic matter content and soil textural class. Their results are presented in Table 4.1

Goldman et al. (1986) note that if site inspection or data analyses indicate significant variations in the soil erodibility, different *K*-factors can be assigned to different areas of the site. They also note that a simpler and more conservative approach is to use the highest value obtained for all parts of the site, because it may not be possible to know exactly what soils will be exposed or how varied the soils are.

For the subbasins of Keramianos, due to the fact that silt is the main element (Chapter 5.2.2) and the percentage of organic matter ranges from 0.7 to 3.5% we chose the soil erodibility factor (*K*) to be 0.45

Table 4.1: Soil Erodibility Factor (after Stewart et al. 1975)

Textural Class	Percentage of Organic Matter		
	<0.5	2	4
Sand	0.05	0.03	0.02
Fine sand	0.16	0.14	0.10
Very finesand	0.42	0.36	0.28
Loamy sand	0.12	0.10	0.08
Loamy finesand	0.24	0.20	0.16
Loamy very fine sand	0.44	0.38	0.30
Sandy loam	0.27	0.24	0.19
Fine sandyloam	0.35	0.30	0.24
Very fine sandy loam	0.47	0.41	0.33
Loam	0.38	0.34	0.29
Silt loam	0.48	0.42	0.33
Silt	0.60	0.52	0.42
Sandy clayloam	0.27	0.25	0.21
Clay loam	0.28	0.25	0.21
Silty clayloam	0.37	0.32	0.26
Sandy clay	0.14	0.13	0.12
Silty clay	0.25	0.23	0.19
Clay		0.13-0.2	

- Cover and Management factor

The USLE cover and management factor C is defined as the ratio of soil loss from land cropped under specified conditions to the corresponding loss from clean-tilled, continuous fallow (Wischmeier and Smith, 1978). The C factor represents the effect of land use on soil erosion (Renard et al., 1997).

By definition, $C = 1$ under standard fallow conditions. As surface cover is added to the soil, the C factor value approaches zero. For example, a C factor of 0.20 signifies that 20% of the amount of erosion will occur compared to continuous fallow conditions. C factors vary from region to region because they are strongly influenced by different R factors (Wischmeier and Smith, 1978). Cover and Management factors chosen for every land use are shown in Table 4.2.

Table 4.2: Selected Cover and Management factors

Land Cover	USLE_C
Apple	0.001
Olives	0.001
Summer Pasture	0.003
Forest - Deciduous	0.001
Forest - Evergreen	0.001
Range Grasses	0.003
Range Brush	0.003
Pine	0.001
Vineyard	0.1
Durum Wheat	0.03
Spring Barley	0.01
Oats	0.03
Spring Wheat	0.03
Green Beans	0.2
Potato	0.2
Tomato	0.03
Carrot	0.2
Sorghum Hay	0.2
Corn Silage	0.2
Alfalfa	0.1
Tobacco	0.2

- Support practice factor

The support practice factor P , is defined as the ratio of soil loss with a specific support practice to the corresponding loss with up-and-down slope culture. Support practices include contour tillage, stripcropping on the contour and terrace systems. It is used to evaluate the

effects of contour tillage, stripcropping, terracing, subsurface drainage and dry – land farm surface roughening.

As mentioned previously (Chapter 3.1.3), the agricultural and rural practices that are exerted in the area, rather hinder the soil loss in the area of Keramianos. Therefore, the support practice factor for the specific subbasins was set equal to the maximum value, equal to 1, and for the rest of the subbasins, it was set to the value of 0.8 according to Karydas et al. (2009), considering that the majority of the area is covered with olives.

- Topographic factor

The topographic factor, LS is the expected ratio of soil loss per unit area from a field slope to that from a 22.1-m length of uniform 9% slope under otherwise identical conditions. The value is determined from topographic maps.

- Coarse fragment factor

The coarse fragment factor can be calculated as $F = \exp(-0.053 \cdot rock)$, where $rock$ is the percent rock in the first soil layer (%). Each soil has different percentages of rock, clay, sand and silt.

4.4.5 Sediment Routing Parameters

- Channel erodibility factor

The channel erodibility factor K_{ch} is conceptually similar to the soil erodibility factor and it is a function of properties of the bed or bank materials. In order for the channel erodibility to be measured, a submerged vertical jet device is used. In our case, for the case of Keramianos, the channel erodibility factor was set equal to 0.6 and 0.3 for the rest of the watershed.

- Channel cover factor

The channel cover factor, C_{ch} , is defined as the ratio of degradation from a channel with a specific vegetative cover to the corresponding degradation from a channel with no vegetative cover. The vegetation affects degradation by reducing the stream velocity, and consequently its erosive power, near the bed surface. For the case of Keramianos, channel cover factor value was set to 1 and for the rest of the watershed 0.2.

- User defined parameters

Peak rate adjusted factor was set to 1.5 after trials and linear and exponent parameter for calculating the maximum amount of sediment that can be reentrained during channel sediment routing were set to 0.00027 and 1.5 respectively.

4.4.6 Discharge simulation

SWAT was run using flow records for the 1973-2014 period. Specifically, the 1973-2010 data were used to calibrate the model (Nikolaidis et al., 2013), whereas the 2010-2014 data were used for model validation. The model discharge was tested for the subbasin of Koiliaris river (Ag. Georgios station) where flow measurements exist.

4.4.7 Suspended Sediment Concentration Simulation

Suspended sediments from Ag. Georgios hydrometric station (H1), monitored between December 2011 and February 2014 using grab samples on a monthly basis, were used for a rough calibration of the model. The sampling point is located just downstream of the cross-section, where the Keramianos tributary, primarily responsible for the sediment transport, merges with the main river, the latter being fed by the karst springs. We can assume that the flow coming from the karst springs has a constant sediment concentration equal to 4 mg/l (according to field measurements). Thus, the sediment concentration at the sampling point is equal to

$$C_{\text{sample}} = \frac{Q_{\text{karst}} * 4 \text{ mg/l} + Q_{\text{surface}} * C_{\text{surf flow}}}{Q_{\text{karst}} + Q_{\text{surf flow}}} \quad (4.30)$$

where Q_{karst} is the flow from the karst springs, $Q_{\text{surf flow}}$ is the surface flow from tributaries (mainly Keramianos) and $C_{\text{surf flow}}$ is the sediment concentration of the surface flow. For the sediment calibration, the sediment concentration from the model given by Equation 4.30 was expected to match the observed values. Suspended sediment concentration measurements were also available from Keramianos from the latest field visits. Therefore, SWAT model output was also tested for the case of Keramianos.

5. RESULTS

5.1 PRELIMINARY RESULTS OF THE SEDIMENT TRAP

We tested the device at Keramianos tributary before entering the gorge during sediment transport events on 2 dates with significant rain events: 4/12/2013 and 2/1/2014. The mean concentration of SSC was 195 and 370 mg/l respectively. During the sampling, the flow was stable, and so was the pumping rate. The device was activated for a specific time period and samples were taken from the river between equal intervals during this period.

Figures 5.1 and 5.2 present the first results of the testing of the device. Specifically, Figure 5.1 shows the testing of the Sediment Trap on the 4/12/2013 and Figure 5.2 presents the testing on the 2/1/2014. Samples were taken manually after a certain volume of river water passed through the device (2 liters in the first case and 1.2 in the second) and a total amount of four samples were collected in each case. The samples were then analyzed in the laboratory for suspended sediment concentration using the techniques described in Chapter 4.2.1 and the concentrations are also presented in Figures 5.1 and 5.2 (blue dots).

The total mass of the suspended sediment in the river, during the sampling, was estimated after applying a quadratic equation on the four samples. The corresponding mass was estimated from the Sediment Trap simply by measuring the mass difference of the pre – weighted filter.

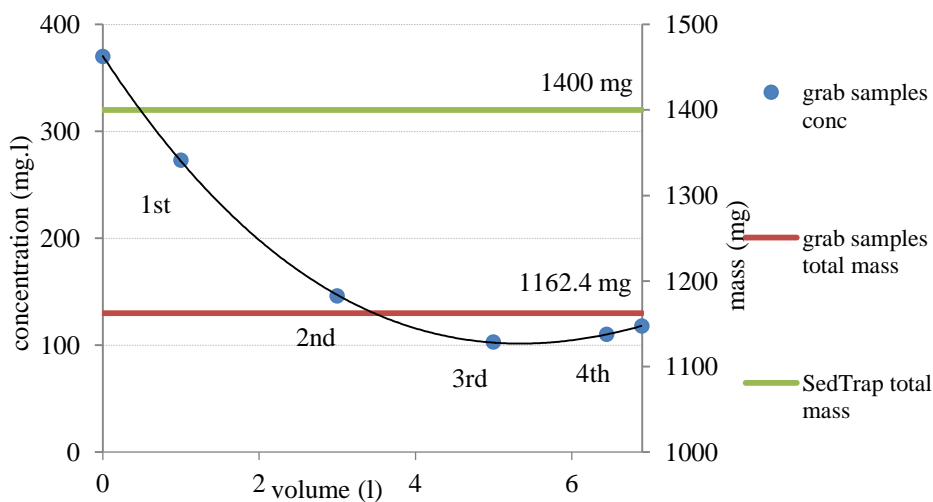


Figure 5.1: First application of the Sediment Trap (4/12/2013)

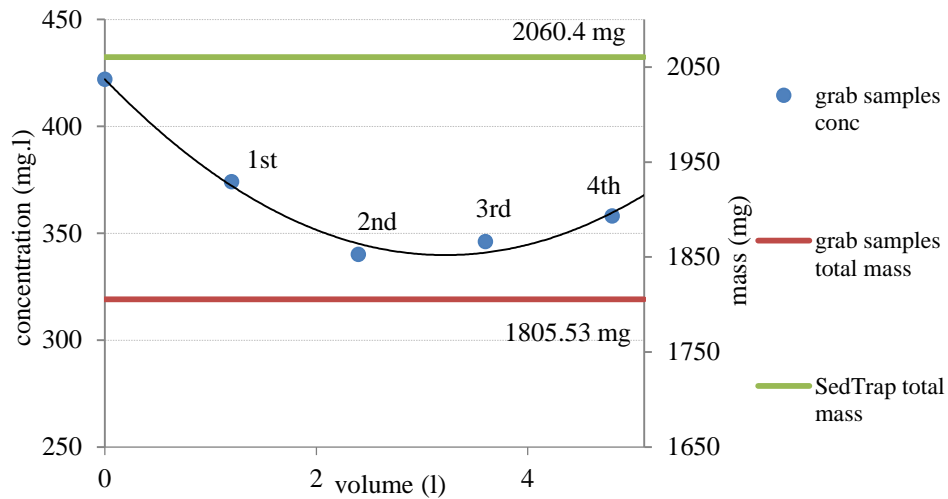


Figure 5.2: Second application of the Sediment Trap (2/1/2014)

On the first trial, the grab samples yielded a total mass of 1200 mg and the total mass that passed through the Sediment trap was equal to 1400 mg (16% error). On the second trial we had a 14% error, with the total mass of grab samples being 1806 mg and the mass that passed through the SedTrap being 2060 mg. The error in the suspended sediment mass is probably due to the orientation of the nozzle, as in both cases it was facing upward, leading to overestimation of the concentration (García, 2008). In any case, the error is considered small, taking the multivariate nature of the river under consideration. Further testing of the device will be accomplished shortly, and such factors will be examined.

5.2 SUSPENDED SEDIMENT ANALYSIS

5.2.1 Grain Size Analysis

Comparison of the distributions of the samples is also presented in Figures 5.3 and 5.4. Specifically, in Figure 5.3 the distributions of the three samples taken from Keramianos are shown, and in Figure 5.4 the distributions of two samples collected on the same day from two different locations (Keramianos tributary and Ag Georgios station) are presented. In both cases, the distributions seem identical.

The results of the statistical analysis on grain size are shown in Table 5.1. Grain-size statistical parameters are given in phi units. Samples are characterized as fine to very fine silt. All the samples appear to be very poorly sorted and skewness analysis showed that their distribution are nearly symmetrical, with the exception of the sample taken from Ag Georgios for which the skewness was negative, meaning a trend towards positive phi values; in other words the particulate sample excesses coarse material in comparison with the rest of the samples. This is quite reasonable, taking under consideration that the Keramianos tributary is enriched with coarser sediment as it flows downstream. Kurtosis shows a state of mesokurtic and leptokurtic distributions. It was also observed that 90% of the sediment has a diameter of over 2 μm . This is the reason why a filter with a pore diameter of 5 μm was chosen, so that the 70% of the sediment could be retained, and a problem of filter clogging would not exist.

Table 5.1: Statistical analysis of grain size for the four samples

Samples	Keramianos 15/11/2013	Keramianos 4/12/2013	Ag. Georgios 4/12/2013	Keramianos 2/1/2013
Mean (phi)	7.13	6.90	6.74	7.09
Median (phi)	7.10	6.85	6.60	7.02
Mode (phi)	6.20	5.90	6.00	6.04
Range (phi)	10.80	12.34	10.80	10.58
Sorting	2.77	2.61	2.60	2.73
Skewness	-0.08	-0.08	-0.19	-0.11
Kurtosis	1.13	0.99	1.08	1.07

The Mann – Whitney test showed that all samples have identical distributions (Table 5.2), thus there is no significant difference between aliquots taken on different dates or from a different location at the 99% confidence level.

Table 5.2: Results of Mann – Whitney test

Combination of Samples	Mann – Whitney test – significance
Keramianos 4/12/2013 - Keramianos 2/1/2014	0.2581
Keramianos 4/12/2013 - Ag Georgios 4/12/2013	0.9655
Keramianos 4/12/2013 - Keramianos 15/11/2013	0.4698
Keramianos 2/1/2014 - Keramianos 15/11/2013	0.6892
Keramianos 2/1/2014 - Ag Georgios 4/12/2013	0.2128
Keramianos 15/11/2013 - Ag Georgios 4/12/2013	0.3908

As far as ANOVA is concerned, the p – value of 0.118, suggested that the null hypothesis could not be rejected (there is no significant difference between the mean values at a 99% confidence level). Thus, it was concluded that samples taken from Keramianos have the same properties with the ones collected at Ag Georgios, and testing the sediment trap at Keramianos tributary is safe for the results.

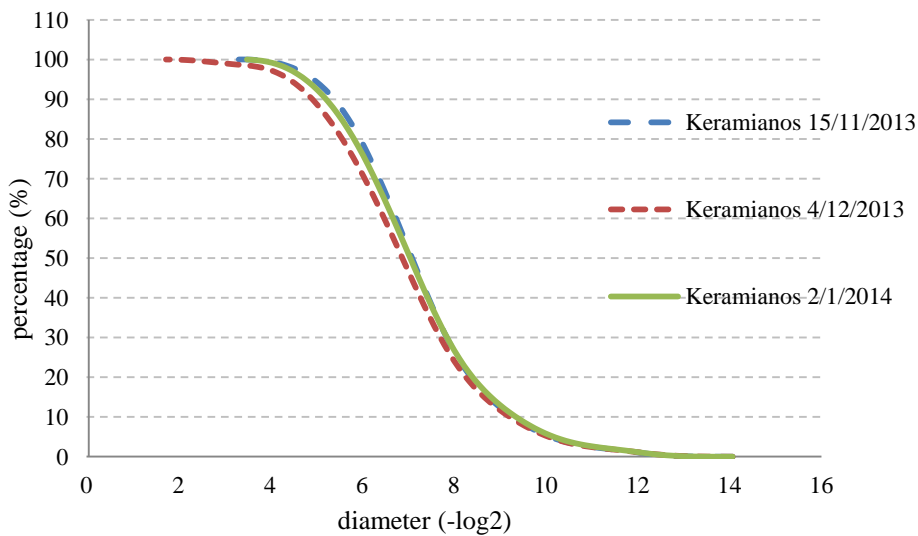


Figure 5.3: Grain size distributions of three samples taken from Keramianos on three different dates

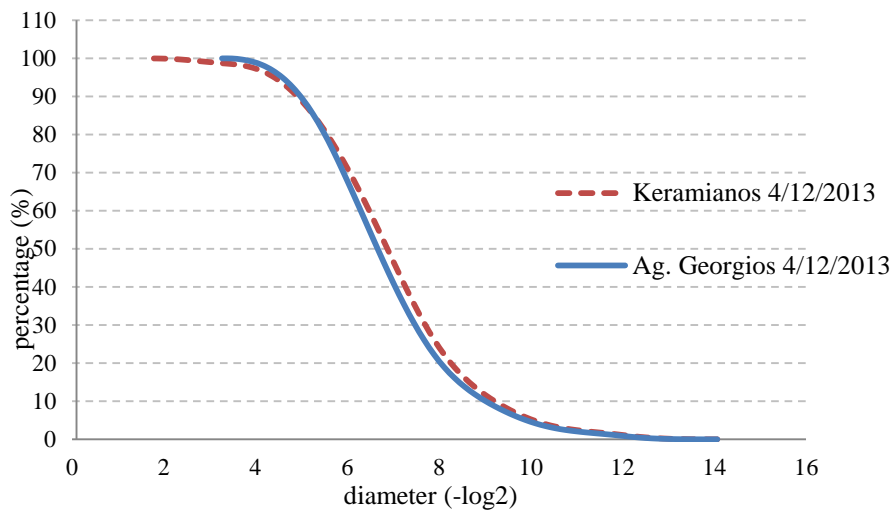


Figure 5.4: Grain size distributions of two samples taken from Keramianos and Ag. Georgios on the same date.

5.2.2 Geochemical Analysis

The XRF analysis results are shown in Table 5.3. For all three samples the results had no significant difference, suggesting similar sediment source. The percentage of SiO₂ is high on account of the abundance of silicate minerals (tertiary sediments, schist). The percentages of K₂O and P₂O₅ indicate fertilizer being washed away. MgO and CaO are indicators of dolomite and limestone and, finally, oxides of Fe and Al contribute to the formation of a hydroxide coating.

These XRF results were also compared with the ones obtained by Moraetis et al.(under review). Moraetis et al. conducted an XRF analysis for various sites of the watershed, each one with different soil types. For the case of schists, that are the main soil in the subbasin of Keramianos, the results of the XRF analysis are shown in Table.5.3, and compared with the results of the XRF analysis for suspended sediment from Keramianos (Figure 5.5). The schist soils, as expected, have high percentages of SiO₂ (igneous rocks), and so do the samples of suspended sediment. The rest of the compounds are also in accordance when compared between soils and suspended sediments, with the exception of CaO. Suspended sediments appear to have significant percentages of CaO due to the fact that the Keramianos tributary flows over a region of limestones, before entering the area covered with schists (Figure 5.5)

Table 5.3: XRF Analysis

Percentages(%)	Na ₂ O	MgO	K ₂ O	CaO	TiO ₂	MnO	Fe ₂ O ₃	Al ₂ O ₃	SiO ₂	P ₂ O ₅
Keramianos 15/11/2013	1.09	2.94	4.56	7.54	1.18	0.09	9.76	23.99	47.22	0.99
Keramianos 4/12/2013	2.46	4.56	1.65	14.46	1.00	0.07	7.54	17.06	50.30	0.56
Keramianos 2/1/2014	1.52	3.21	2.87	12.06	1.09	0.10	9.55	21.71	44.97	0.83
Schists in the area	0.00		0.50	0.10	0.50		6.00	7.20	81.3	0.10

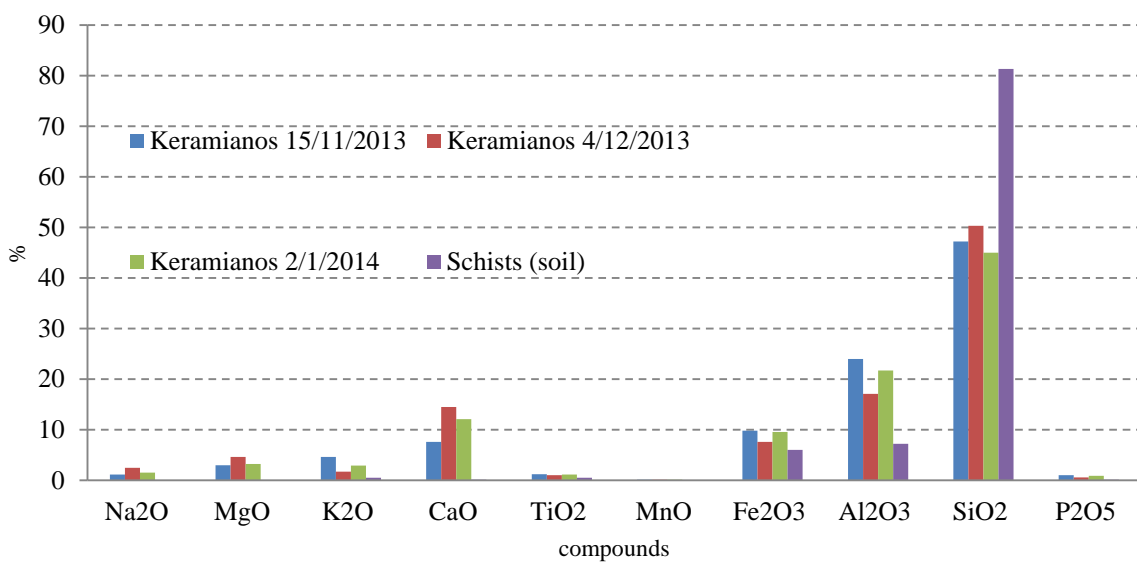


Figure 5.5: Depiction of outcomes of XRF Analysis of suspended sediment samples and the schist soil of the area.

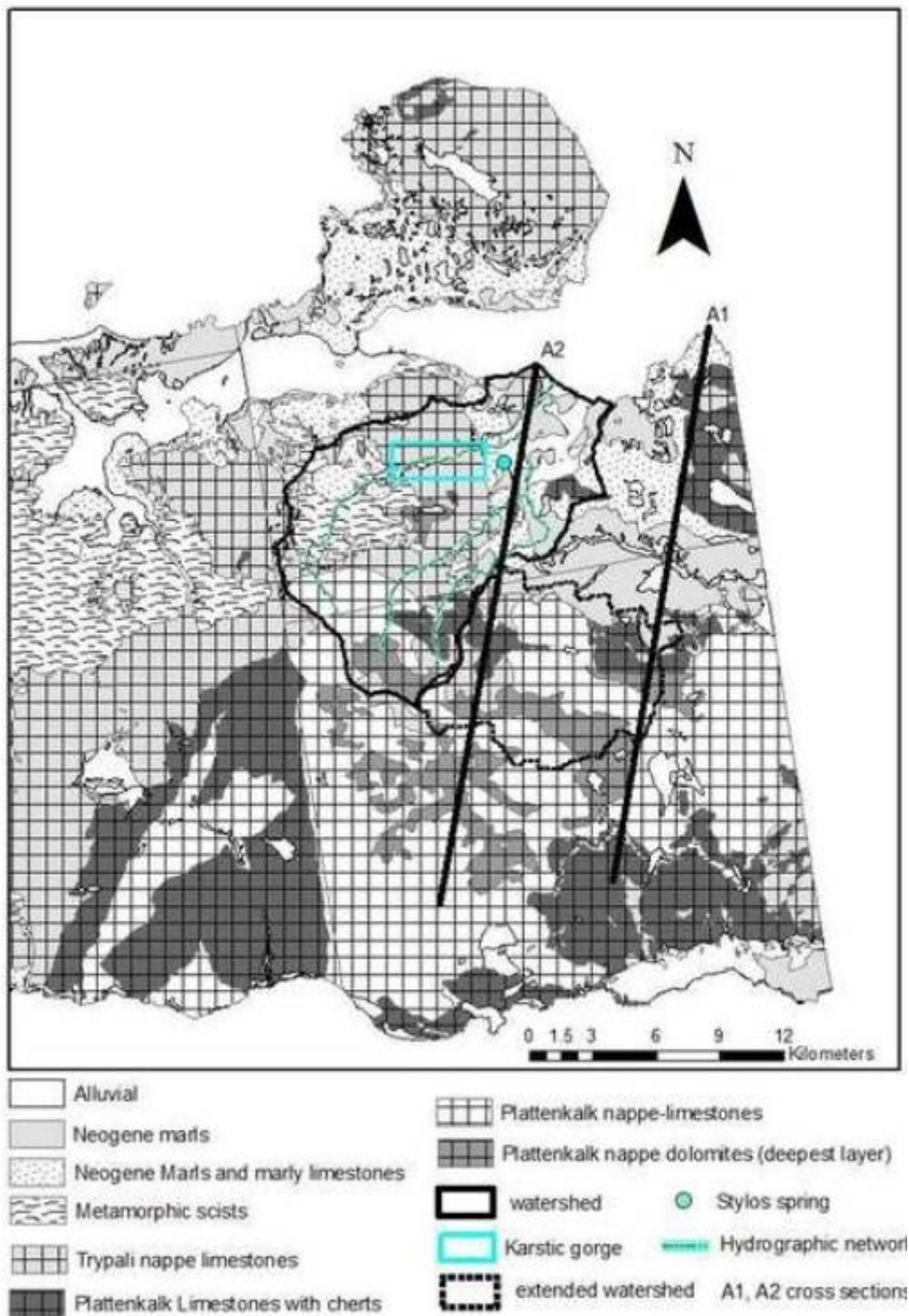


Figure 5.6: Geologic map of Koiliaris River basin boundary and estimated extended karst area (Nikolaidis et al., 2013)

5.2.3 Turbidity – suspended sediment concentration curve

A total of 20 samples were collected and the results are plotted in Figure 5.7. Two of the samples were taken from Ag. Georgios station and were in good agreement with the samples taken from Keramianos, suggesting that suspended sediment particle size and properties are maintained even after the exit of Keramianos from the gorge. The empirical curve obtained was the following:

$$SSC = 0.502 \cdot turb \quad (5.1)$$

where SSC is the suspended sediment concentration (mg/l) and turb is the turbidity (NTU). The coefficient of determination is equal to 0.98 (the line was forced through the origin to avoid negative suspended sediment outputs), which is considered to be very good (Moriassi et al., 2007). Measurements of the spectrophotometer were found to be consistent with turbidity measurements ($r^2 = 0.98$ as opposed to filtration with $r^2 = 0.92$), which is reasonable, taking into consideration that the porosity of the filters used was 2 – 3 μm and the suspended sediment is considerably fine (see Chapter 5.2.1). The establishment of the curve has not been completed yet, since more samples are needed for more robust results.

Turbidity is monitored at Ag. Georgios station every five minutes. Thus, using the above mentioned curve, in combination with the turbidity measurements that are recorded in situ, an overview of the concentration distribution during the phenomenon will be available.

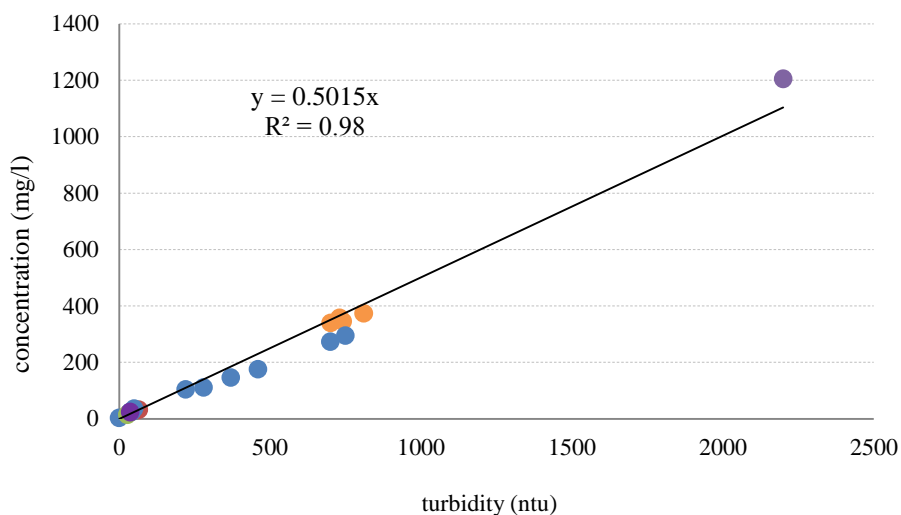


Figure 5.7: Turbidity – Suspended Sediment Concentration curve

5.3 SWAT MODELING

The region surrounding Koiliaris River basin was delineated into 41 sub-basins. Koiliaris River basin has a surface area of 132 km² and was divided into 11 subbasins.

5.3.1 Discharge simulation

SWAT was run using flow records for the 1973-2014 period. Specifically, the 1973-2010 data were used to calibrate the model, whereas the 2010-2013 data were used for model validation. Figure 5.8 depicts simulated flows versus the observed data at Ag Georgios for the 2004-2014 period, during which continuous daily flow data were available.

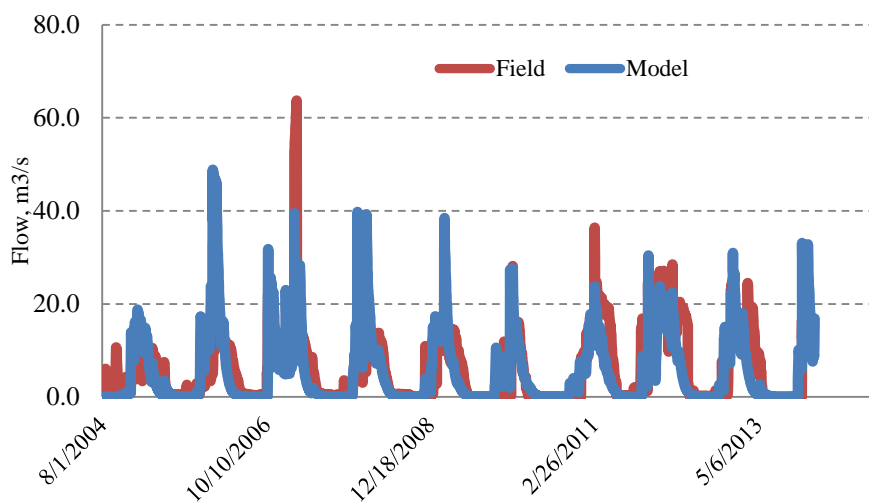


Figure 5.8: Hydrologic Simulation at Ag. Georgios station for the 2004-2014 period

The simulation results suggest that the model can adequately describe the hydrology of the watershed. The goodness of fit of the calibration was tested against three statistical metrics proposed by Moriasi et al. (2007): the Nash-Sutcliffe Efficiency (NSE), Percent Bias (PBias), and RMSE Standard Deviation Error (RSR). A simulation is considered adequate if $NSE > 0.5$, $Pbias < 25\%$ and $RSR < 0.7$. For the 1973-2010 validation period, the NSE was 0.8, PBias 25.3% and RSR 0.45 for the daily records and 0.83, 23.4% and 0.41 for the monthly records, respectively. The goodness of fit of the calibration was considered adequate since all three error metrics were acceptable for both daily and monthly records. The discharge root mean square error (RMSE) was estimated to be 5.7 m³/s and the closure of the cumulative simulated flow for the validation period and observed flow was 25%, while the correlation coefficient between observed and simulated flows was 0.62 and the slope 0.68.

5.3.2 Suspended sediment simulation

Sediment concentration measurements from grab samples taken at Ag Georgios station (2011-2014) were used for the calibration of the model's sediment concentration simulations. There is good agreement between simulated and observed concentration values as depicted in the semi-logarithmic diagram of Figure 5.9, considering that the available concentration data were limited to low concentration values and there was only one observation available during flood conditions. However, it is a fact that, once or twice a year, during flood conditions, Keramianos tributary transfers significant loads of suspended sediment. The objective was to calibrate the sediment in such a way that high suspended sediment concentrations (originating from the subbasins with schist formations) would be simulated, and at the same time, the model output would match the available low concentration values, using equation (4.16).

For the 2011-2014 period, the NSE was 0.7, the PBias - 57% and RSR - 0.55 for the daily records. The goodness of fit of the calibration was considered adequate since the two error metrics were acceptable. The PBIAS did not have an acceptable value, and revealed model overestimation; but considering the fact that the majority of the observations had low values (4 mg/l) and only one observation exceeded 100 mg/l (300 mg/l on 4/12/2013), the metric was biased in favor of the error resulting from this high value. The suspended sediment concentration root mean square error (RMSE) was estimated to be 0.32 mg/l, while the correlation coefficient between observed and simulated flows was 0.99 and the slope 1.53.

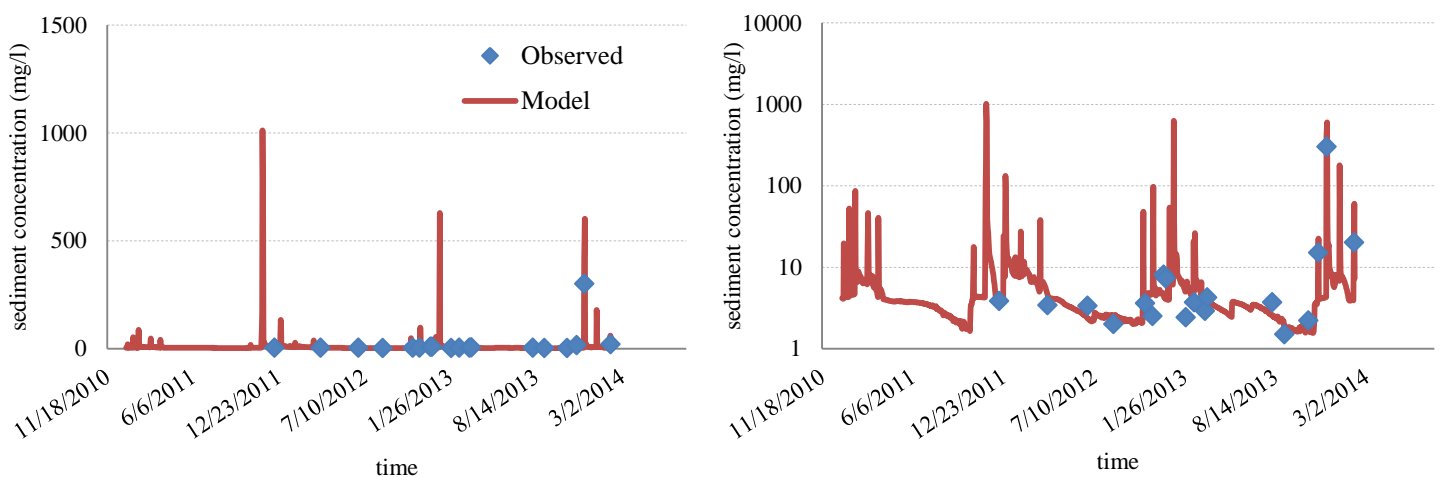


Figure 5.9 Suspended Sediment Simulation for Ag. Georgios station a) normal axes b) logarithmic y axis

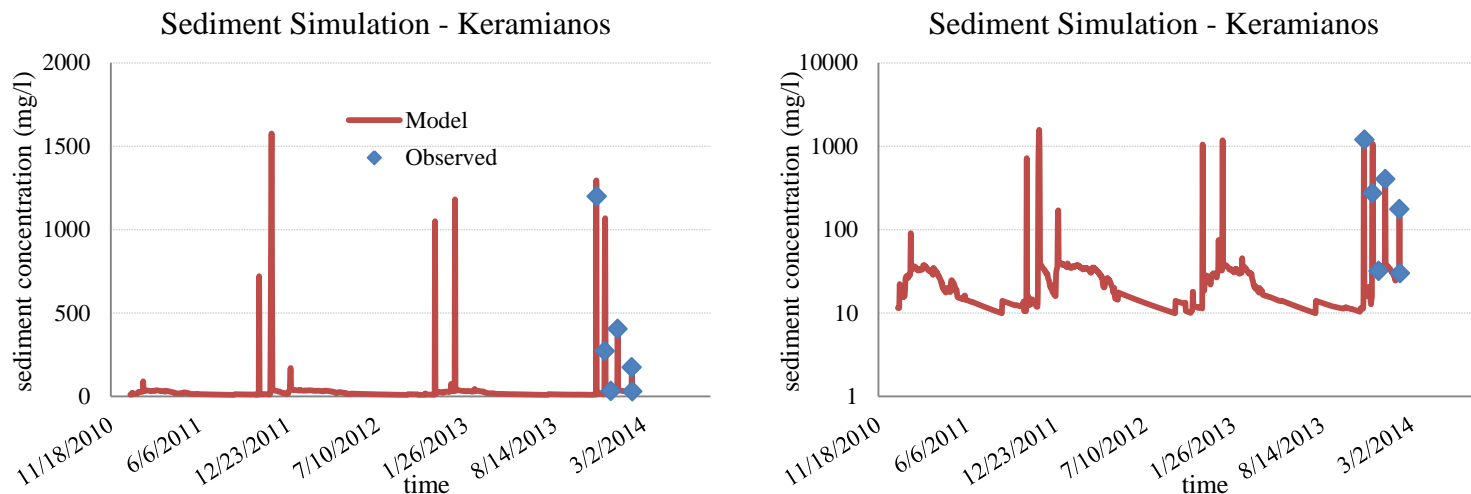


Figure 5.10: Suspended Sediment Simulation for Keramianos tributary a) normal axes b) logarithmic y axis

Suspended sediment simulation was also tested for the tributary of Keramianos. Only six observations were available, therefore no testing against statistical meters was conducted. However, the model has a good response in both low and high concentrations (Figure 5.10). The fact that the model seems to overestimate concentration in some cases (e.g. on 4/12/2013), may be due to the fact that the SSC is temporally variable, and the sampling at that instant was not representative. Using the results of the model, it is estimated that during a flood event, the Keramianos tributary transports 95% of the sediment mass.

When the implementation of the automated sampling system will be completed, turbidity data recorded at Ag. Georgios station will be used to “generate” more suspended sediment concentration data and to further calibrate the model.

5.3.3 Erosion and sediment export

After the calibrated SWAT model was run, an output of daily sediment yield from each subbasin was available. Aggregation of this output on an annual basis, resulted in maps revealing the subbasins with the highest erosion yields, stating the highest erosion rates. In Figure 5.7 the mean annual erosion rate for the extended watershed of Koiliaris is depicted. It is obvious that the subbasin of Keramianos is the one with the highest sediment yield, thus the highest erosion rate (0.75 metric tons/ha/year). Figures 5.12 and 5.13 present the annual erosion rate of Koiliaris watershed on a wet and dry year respectively.

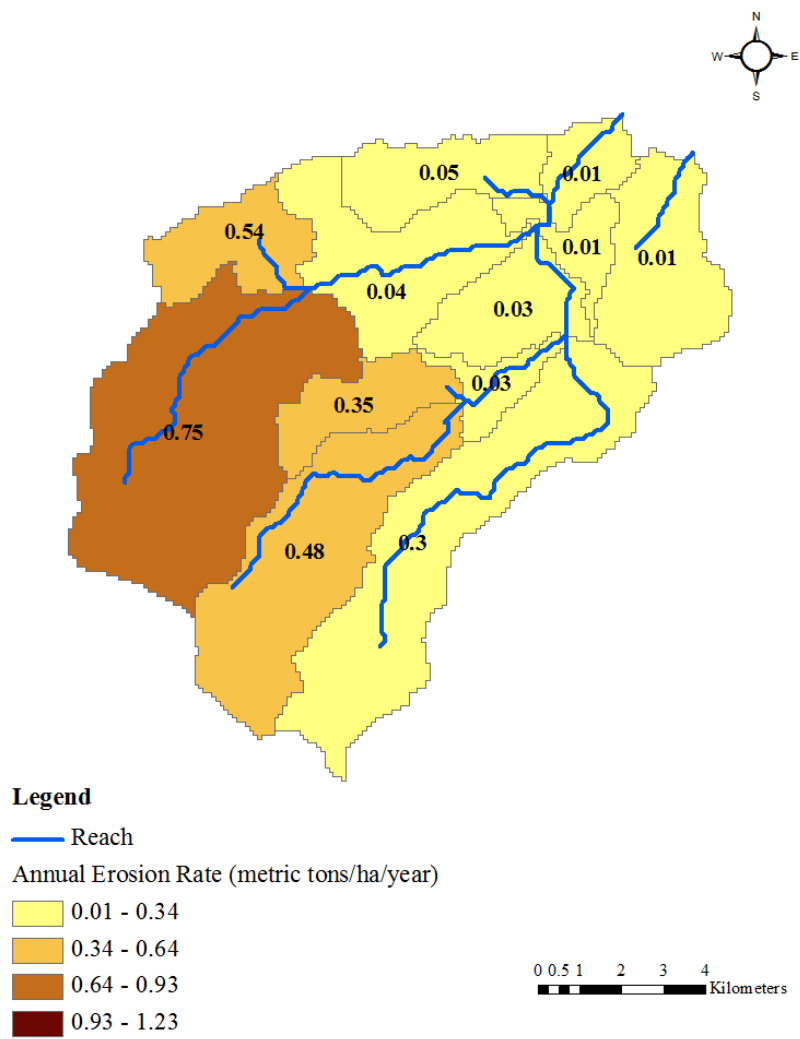


Figure 5.11: Mean Annual Erosion rate for the watershed of Koiliaris

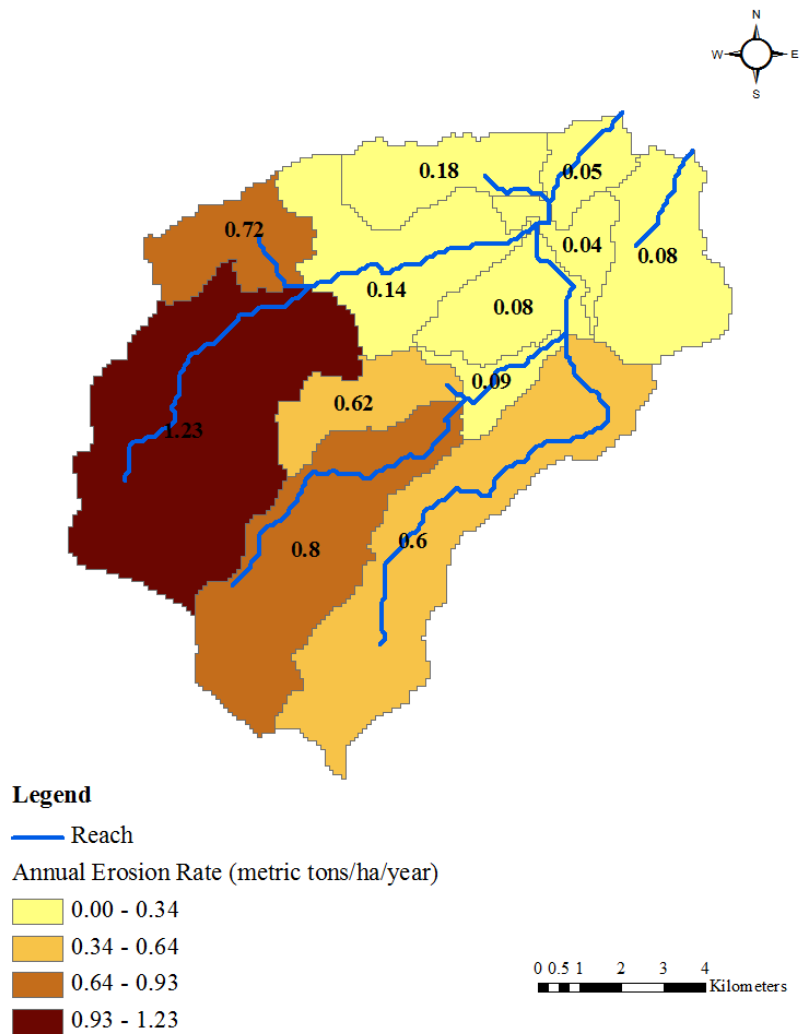


Figure 5.12: Annual Erosion rate for the watershed of Koiliaris on a wet year

On a wet year (Figure 5.12), the contribution of the subbasin of Keramianos in the sediment yield is 1.23 metric tons/ha/year and on a dry year (Figure 5.13), the erosion rate is significantly lower (0.24 metric tons/ha/year).

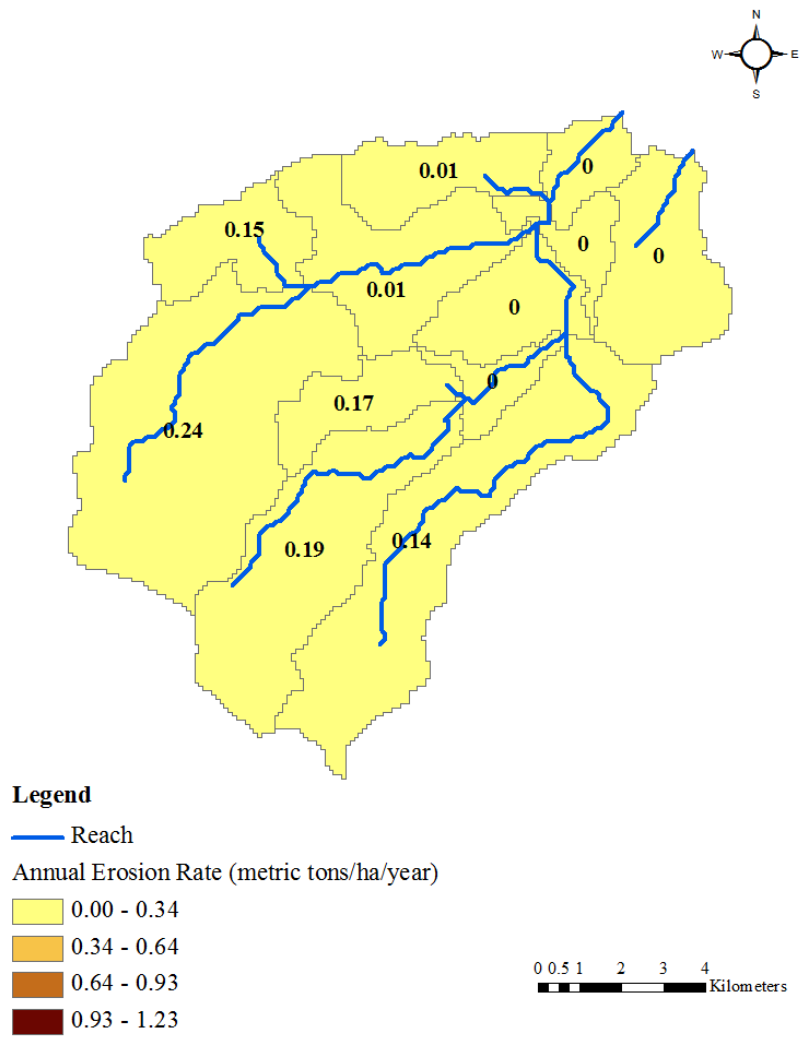


Figure 5.13: Annual Erosion rate for the watershed of Koiliaris on a dry year

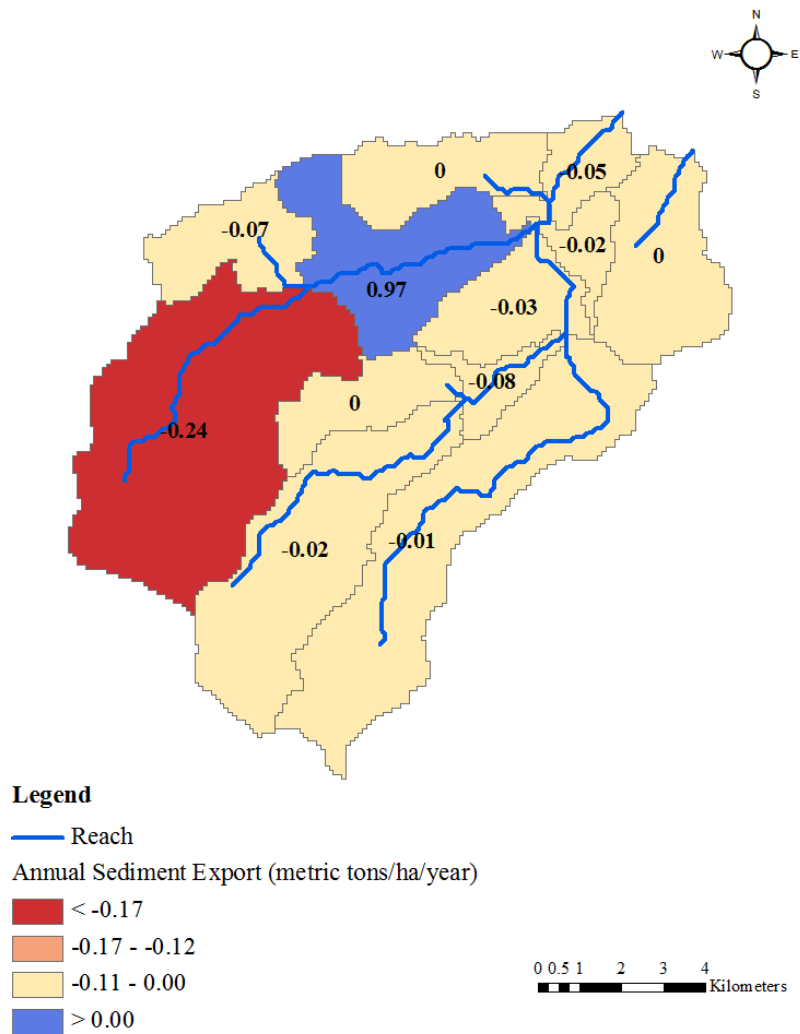


Figure 5.14: Mean Annual Sediment Export for the watershed of Koiliaris

According to SWAT, the subbasin of Keramianos “loses” 0.24 metric tons/ha/year, and the subbasin of Koiliaris (at Ag. Georgios station) is enriched with a ratio of 0.97 metric tons/ha/year (Figure 5.14). On a wet year (Figure 5.15) the export of sediment to the sea is estimated to be about 9324 tons/year and the subbasin of Keramanos is responsible for the 70% of it. On the other hand, on a dry year (Figure 5.16) 1958 tons/year are exported to the sea, and Keramianos is responsible for the 33% of it.

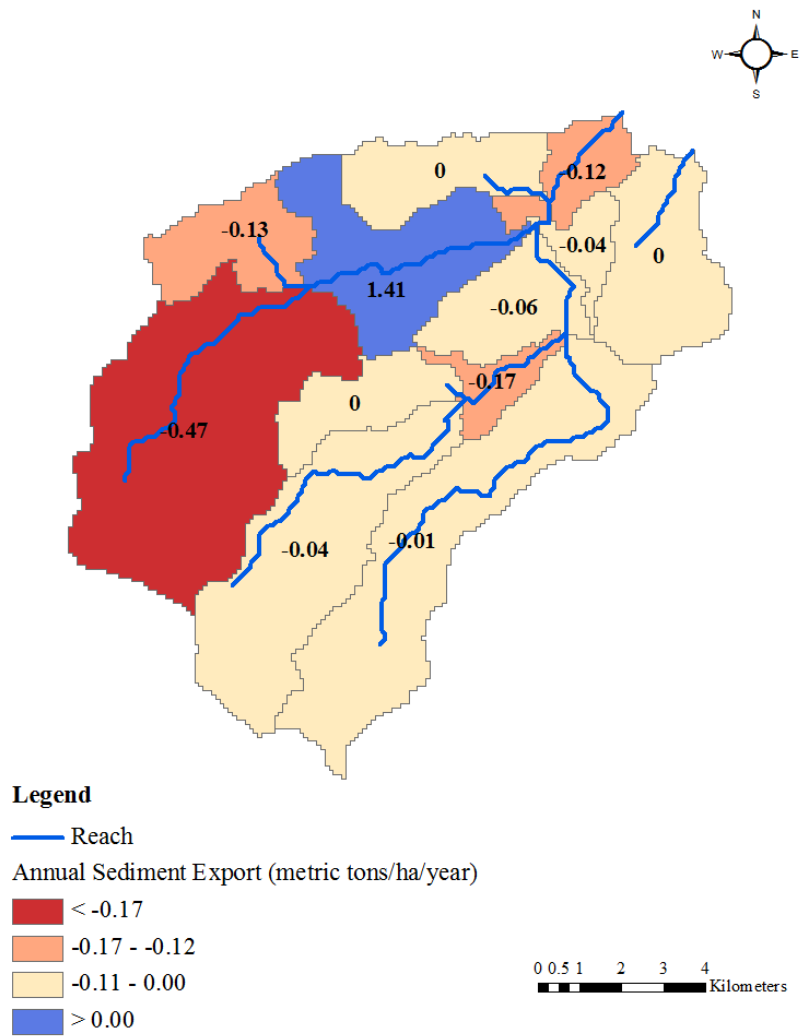


Figure 5.15: Mean Annual Sediment Export for the watershed of Koiliaris on a wet year

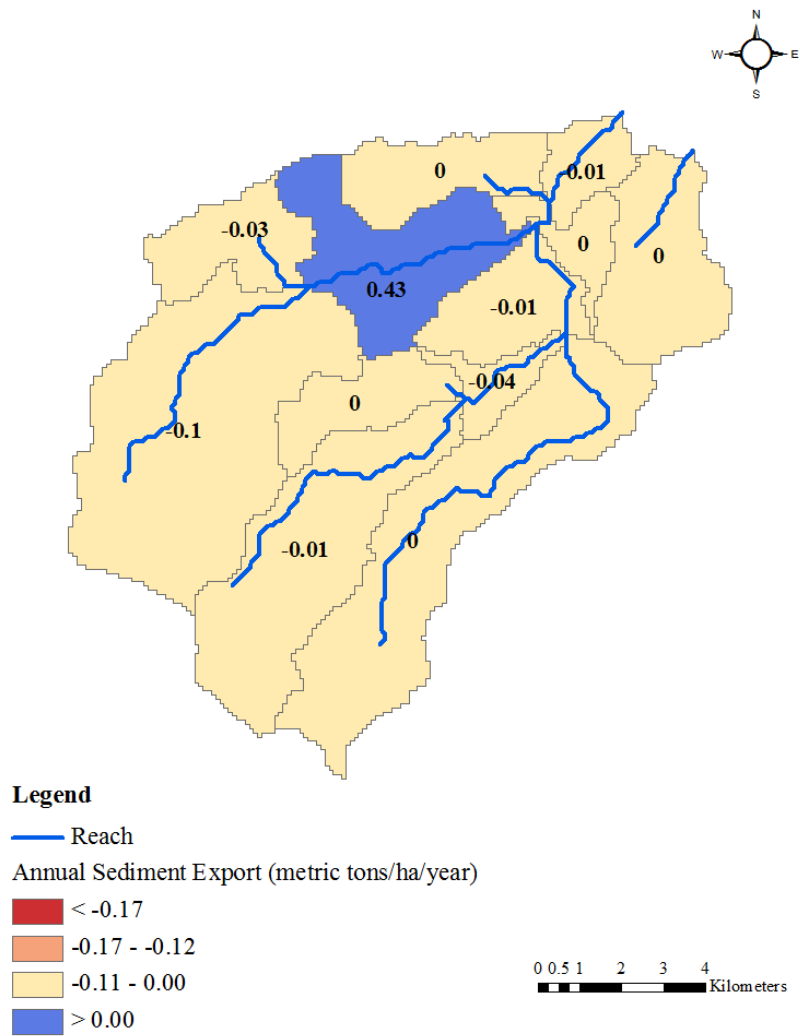


Figure 5.16: Mean Annual Sediment Export for the watershed of Koiliaris on a dry year

6 CONCLUSIONS

In this thesis a methodology was developed to estimate the suspended sediment fluxes of Koiliaris river basin in Crete. The methodology consisted of a combination of monitoring, analysis and modeling tools that would bridge the data gap of suspended sediment yield in Mediterranean rivers.

The methods that were applied for the purposes of this study can be divided into three major sections:

- Sampling and Monitoring:

Sampling for suspended sediment in the Koiliaris river basin, up to now, was conducted with grab sampling, a method that only provides a rough estimation of sediment transport. The grab samples that were available, provided only low suspended sediment concentrations, a characteristic of the karst springs, and no data were available from flash floods, when high sediment loads are transferred. Therefore, as part of this study, an automated – pump operated – sampling device is proposed. The device initiates sampling when certain thresholds of water stage or turbidity are met. Sampling is performed via an intake nozzle, and pump rotation is proportional to the flow; water flow is deducted indirectly from stage, with the use of a rating curve, created for the specific sampling point.

The device is currently undergoing testing. For the first trials, the results were satisfactory: the error was 15 and 14% respectively, and the Sediment Trap overestimated the total suspended sediment mass compared to the mass deducted from the simultaneous grab sampling. The error can be justified by the orientation of the nozzle, as in both cases it was facing upward, leading to overestimation of the concentration. The trials were performed at Keramianos tributary, therefore, in order to certify that the suspended sediment there has the same properties with the suspended sediment at Ag Georgios, suspended sediment analysis was conducted.

- Suspended Sediment Analysis

Suspended sediment analysis includes Grain Size Analysis, Geochemical Analysis and the establishment of a “Turbidity – Suspended Sediment Concentration” curve.

- Grain Size analysis revealed the grain size distributions of the suspended sediment samples and was used for the comparison of samples of different time instants and sampling points. As the distributions were not normal, Mann – Whitney test was applied

to test whether pairs of distributions were identical. The Mann – Whitney test showed that all samples are of an identical distribution. In order for the mean values of the samples that were taken from different locations to be compared, each $\Phi 50$ value was considered as a sample and the average $\Phi 50$ of the samples collected from Keramianos, were compared with the ones from Ag Georgios using the analysis of variance (ANOVA). The p – value of 0.118, suggested that the null hypothesis could not be rejected (there is no significant difference between the mean values at a 99% confidence interval). Thus, it was concluded that specimens taken from Keramianos have the same properties with the ones collected at Ag Georgios, and testing the sediment trap at Keramianos tributary is safe for the results.

- Geochemical Analysis included XRF (X – Ray fluorescence analysis) applied for three samples taken from Keramianos tributary. The percentage of SiO_2 was high on account of the abundance of silicate minerals (tertiary sediments, schist). XRF analysis results for the schist soil of the area were in good agreement with the ones for the suspended matter.
- An empirical relationship between turbidity and suspended sediment concentration was developed in order to establish the sampling conditions of the Sediment Trap. Samples were taken under various conditions of suspended sediment concentrations with a simultaneous measurement of in field turbidity. The empirical curve obtained was the following: $SSC = 0.502 \cdot turb$. The coefficient of determination is equal to 0.98, which is considered to be very good. In addition, the fact that the curve included samples from both Ag. Georgios and Keramianos shows that samples from both fields are in good agreement.
- Modeling of Suspended Sediment

Modeling of suspended sediment was performed with the Sediment Component of SWAT model, after having simulated the hydrology of the watershed.

- The simulation of the hydrology was validated for the years 2010 to 2014 and the results suggest that the model can adequately describe the hydrology of the watershed; three statistical metrics proposed by Moriasi et al. (2007) were applied to test the goodness of fit of the simulation, and all of them were passed for both daily and monthly record.
- For the simulation of the suspended sediment concentration, the model was calibrated in such a way so that the suspended sediment transport would originate from the subbasin of Keramianos. The simulation was validated with suspended sediment values from grab sampled taken from both Ag. Georgios and Keramianos. For the case of Ag Georgios the

results were satisfactory, and the goodness of fit of the simulation was tested with the three statistical metrics mentioned above. For the case of Keramianos, the available measurements were limited, but still the observed values were in good agreement with the simulation. According to the results, 95% of the sediment mass during a flood event originates from the Keramianos tributary. Finally, using the suspended sediment concentration output of the model, maps which depict the erosion sources and the total sediment export were constructed.

References

- Abtew, W., B. Powell, and South Florida Water Management District Environmental Monitoring & Assessment. 2003. Cost-Effective Water Quality Sampling Scheme for Variable Flow Canals at Remote Sites. South Florida Water Management District.
- Agrawal, Y. C., and H. C. Pottsmith. 1994. "Laser Diffraction Particle Sizing in STRESS." *Continental Shelf Research* 14 (10–11): 1101–21. doi:10.1016/0278-4343(94)90030-2.
- Agrawal, Y.C., H. C. Pottsmith, J. Lynch, and J. Irish. 1996. "Laser Instruments for Particle Size and Settling Velocity Measurements in the Coastal Zone." In *OCEANS '96. MTS/IEEE. Prospects for the 21st Century. Conference Proceedings*, 3:1135–1142 vol.3. doi:10.1109/OCEANS.1996.569062.
- Alvarez, Moisés. 1990. "Glass Disk Fusion Method for the X-Ray Fluorescence Analysis of Rocks and Silicates." *X-Ray Spectrometry* 19 (4): 203–6. doi:10.1002/xrs.1300190410.
- Arnold, J. G., R. Srinivasan, R. S. Muttiah, and J. R. Williams. 1998a. "Large Area Hydrologic Modeling and Assessment Part I: Model Development1." *JAWRA Journal of the American Water Resources Association* 34 (1): 73–89. doi:10.1111/j.1752-1688.1998.tb05961.x.
- Arnold, J.G., R. Srinivasan, R.S. Muttiah, and J.R. Williams. 1998b. "Large Area Hydrologic Modeling and Assessment Part I: Model Development." *Journal of the American Water Resources Association* 34 (1): 73–89.
- Baier, V., and W. Bechteler. 1996. "An Underwatervideomicroscope to Determine the Size And Shape of Suspended Particles By Means of Digital Image Processing." *The Sixth International Offshore and Polar Engineering Conference*, January.
- Baker, Edward T. and Lavelle, J. William. 1984. "The Effect of Particle Size on the Light Attenuation Coefficient of Natural Suspensions." *Journal of Geophysical Research*. 89(C5):8197-8203
- Bartram, Jamie, and Richard Ballance. 1996. *Water Quality Monitoring: A Practical Guide to the Design and Implementation of Freshwater Quality Studies and Monitoring Programmes*. CRC Press.
- Bennett, James P. 1974. "Concepts of Mathematical Modeling of Sediment Yield." *Water Resources Research* 10 (3): 485–92. doi:10.1029/WR010i003p00485.

- Berke, B. and Rakoczi, L. 1981. "Latest Achievements in the Development of Nuclear Suspended Sediment Gauges." *Erosion & Sediment Transport Measurement (Symposium)*. Florence Italy. IAHS pub. no. 133 pp. 83-90.
- Betrie, G.D., Y.A. Mohamed, A. Van Griensven, and R. Srinivasan. 2011. "Sediment Management Modelling in the Blue Nile Basin Using SWAT Model." *Hydrology and Earth System Sciences* 15 (3): 807–18. doi:10.5194/hess-15-807-2011.
- Black, K. P., and M. A. Rosenberg. 1994. "Suspended Sand Measurements in a Turbulent Environment: Field Comparison of Optical and Pump Sampling Techniques." *Coastal Engineering* 24 (1–2): 137–50. doi:10.1016/0378-3839(94)90030-2.
- Bogen, Jim, Tharan Fergus, and D. E. Walling. 2003. *Erosion and Sediment Transport Measurement in Rivers: Technological and Methodological Advances*. IAHS.
- Cerdan, O., G. Govers, Y. Le Bissonnais, K. Van Oost, J. Poesen, N. Saby, A. Gobin, et al. 2010. "Rates and Spatial Variations of Soil Erosion in Europe: A Study Based on Erosion Plot Data." *Geomorphology* 122 (1-2): 167–77. doi:10.1016/j.geomorph.2010.06.011.
- Clarke, Allan Lawrence, and P. B. Wylie. 1997. *Sustainable Crop Production in the Sub-Tropics: An Australian Perspective*. Department of Primary Industries.
- Clifford, N. J., Richards, K. S., Brown, R. A. and Lane, S. N. 1995. "Laboratory and Field Assessment of an Infrared Turbidity Probe and its Response to Particle Size and Variation in Suspended Sediment Concentration." *Hydrological Sciences*. 40(6):771-791.
- Cohen, S., A.J. Kettner, J.P.M. Syvitski, and B.M. Fekete. 2013. "WBMsed, a Distributed Global-Scale Riverine Sediment Flux Model: Model Description and Validation." *Computers and Geosciences* 53: 80–93. doi:10.1016/j.cageo.2011.08.011.
- Cohen, Sagy, Albert J. Kettner, James P. M. Syvitski, and Balázs M. Fekete. 2013. "WBMsed, a Distributed Global-Scale Riverine Sediment Flux Model: Model Description and Validation." *Computers & Geosciences* 53 (April). *Modeling for Environmental Change*: 80–93. doi:10.1016/j.cageo.2011.08.011.
- Conner, C. S. and DeVisser, A. M. 1992. "A Laboratory Investigation of Particle Size Effects on an Optical Backscatterance Sensor." *Marine Geology*. 10:151-159.
- Crawford, A. M., and Alex E. Hay. 1993. "Determining Suspended Sand Size and Concentration from Multifrequency Acoustic Backscatter." *The Journal of the Acoustical Society of America* 94 (6): 3312–24. doi:10.1121/1.407237.

- Crickmore, M. J., Tazioli, G. S., Appleby, P.G., Oldfield, F. 1990. *The Use of Nuclear Techniques in Sediment Transport and Sedimentation Problems*. Unesco, Paris.
- D & A Instrument Company. 1991. *Instruction Manual for OBS-1 & 3*. D & A Instrument Company, 40-A Seton Road, Port Townsend, WA, 98368.
- De Roo, A. P. J., C. G. Wesseling, and C. J. Ritsema. 1996. "Lisem: A Single-Event Physically Based Hydrological and Soil Erosion Model for Drainage Basins. I: Theory, Input and Output." *Hydrological Processes* 10 (8): 1107–17. doi:10.1002/(SICI)1099-1085(199608)10:8<1107::AID-HYP415>3.0.CO;2-4.
- De Vente, J., J. Poesen, and G. Verstraeten. 2005. "The Application of Semi-Quantitative Methods and Reservoir Sedimentation Rates for the Prediction of Basin Sediment Yield in Spain." *Journal of Hydrology* 305 (1-4): 63–86. doi:10.1016/j.jhydrol.2004.08.030.
- De Vente, J., J. Poesen, G. Verstraeten, A. Van Rompaey, and G. Govers. 2008. "Spatially Distributed Modelling of Soil Erosion and Sediment Yield at Regional Scales in Spain." *Global and Planetary Change* 60 (3-4): 393–415. doi:10.1016/j.gloplacha.2007.05.002.
- De Vente, J., R. Verduyn, G. Verstraeten, M. Vanmaercke, and J. Poesen. 2011. "Factors Controlling Sediment Yield at the Catchment Scale in NW Mediterranean Geoecosystems." *Journal of Soils and Sediments* 11 (4): 690–707. doi:10.1007/s11368-011-0346-3.
- De Vente, Joris, Jean Poesen, Gert Verstraeten, Gerard Govers, Matthias Vanmaercke, Anton Van Rompaey, Mahmood Arabkhedri, and Carolina Boix-Fayos. 2013. "Predicting Soil Erosion and Sediment Yield at Regional Scales: Where Do We Stand?" *Earth-Science Reviews* 127 (December): 16–29. doi:10.1016/j.earscirev.2013.08.014.
- Delmas, M., O. Cerdan, J.-M. Mouchel, and M. Garcin. 2009. "A Method for Developing a Large-Scale Sediment Yield Index for European River Basins." *Journal of Soils and Sediments* 9 (6): 613–26. doi:10.1007/s11368-009-0126-5.
- Desmet, P.J.J., and G. Govers. 1996. "A GIS Procedure for Automatically Calculating the USLE LS Factor on Topographically Complex Landscape Units." *Journal of Soil and Water Conservation* 51 (5): 427–33.
- Downing, Andrew, Peter D. Thorne, and Christopher E. Vincent. 1995. "Backscattering from a Suspension in the near Field of a Piston Transducer." *The Journal of the Acoustical Society of America* 97 (3): 1614–20. doi:10.1121/1.412100.

- Eads, Rand E., and Robert B. Thomas. 1983. "Evaluation of a Depth Proportional Intake Device for Automatic Pumping Samplers." *Water Resources Bulletin* 19 (2): 289–92.
- Folk, R. L., and W. C. Ward. 1957. "Brazos River Bar [Texas]; a Study in the Significance of Grain Size Parameters." *Journal of Sedimentary Research* 27 (1): 3–26. doi:10.1306/74D70646-2B21-11D7-8648000102C1865D.
- Folk, Robert L. 1966. "A Review of Grain-Size Parameters." *Sedimentology* 6 (2): 73–93. doi:10.1111/j.1365-3091.1966.tb01572.x.
- García, M. 2014. "ASCE Manual of Practice 110 — Sedimentation Engineering: Processes, Measurements, Modeling and Practice." In *World Environmental and Water Resource Congress 2006*, 1–4. American Society of Civil Engineers. Accessed March 21.
- Gardner, Robert B. 1993. *A Statistical Analysis of Sand Grain Size in San Salvador, Bahamas*. Bahamian Field Station.
- Gippel, Christopher James. 1995. "Potential of Turbidity Monitoring for Measuring the Transport of Suspended Solids in Streams." *Hydrological Processes* 9 (1): 83–97. doi:10.1002/hyp.3360090108.
- Gippel, Christopher James, Australian Defence Force Academy, and Department of Geography and Oceanography. 1989. *The Use of Turbidity Instruments to Measure Stream Water Suspended Sediment Concentration*. Campbell, ACT, Australia: Dept. of Geography and Oceanography, University College, the University of New South Wales, Australian Defence Force Academy.
- Goldman, Steven J, Katharine Jackson, and Taras A Bursztynsky. 1986. *Erosion and Sediment Control Handbook*. New York: McGraw-Hill.
- Green, Malcolm O., and John D. Boon III. 1993. "The Measurement of Constituent Concentrations in Nonhomogeneous Sediment Suspensions Using Optical Backscatter Sensors." *Marine Geology* 110 (1–2): 73–81. doi:10.1016/0025-3227(93)90106-6.
- Guy, H. P. 1965. *Techniques of Water -Resources Investigations of the United States Geological Survey-Laboratory Theory and Methods for Sediment Analysis*. United States Department of the Interior, United States Geological Survey.
- Haan, C. T, Billy J Barfield, and J. C Hayes. 1994. *Design Hydrology and Sedimentology for Small Catchments*. San Diego, Calif.: Academic Press.

- Hairsine, P. B., and C. W. Rose. 1992. "Modeling Water Erosion due to Overland Flow Using Physical Principles: 2. Rill Flow." *Water Resources Research* 28 (1): 245–50. doi:10.1029/91WR02381.
- Hanes, D. M., C. E. Vincent, D. A. Huntley, and T. L. Clarke. 1988. "Acoustic Measurements of Suspended Sand Concentration in the C2S2 Experiment at Stanhope Lane, Prince Edward Island." *Marine Geology* 81 (1–4): 185–96. doi:10.1016/0025-3227(88)90025-4.
- Henkel, Ramon E. 1976. *Tests of Significance*. SAGE Publications.
- Hicks, D. Murray, Basil Gomez, and Noel A. Trustrum. 2000. "Erosion Thresholds and Suspended Sediment Yields, Waipaoa River Basin, New Zealand." *Water Resources Research* 36 (4): 1129–42. doi:10.1029/1999WR900340.
- Inokuchi, Masao, and Shigekazu Mezaki. 1974. "Analysis of the Grain Size Distribution of Bed Material in Alluvial Rivers." *Geographical Review of Japan* 47 (9): 545–56.
- Inter-agency Committee on Water Resources, Subcommittee on Sedimentation. 1963. *A Study of Methods Used in Measurement and Analysis of Sediment Loads in Streams-Report No. 14 Field Practice and Equipment Used in Sampling Suspended Sediment Report #14*. St. Anthony Falls Hydraulic Laboratory.
- J. Swithenbank, J. M. Beer. 1975. "A Laser Diagnostic Technique for the Measurement of Droplet and Particle Size Distribution" -1.
- Karydas, Christos G., Tijana Sekuloska, and Georgios N. Silleos. 2009. "Quantification and Site-Specification of the Support Practice Factor When Mapping Soil Erosion Risk Associated with Olive Plantations in the Mediterranean Island of Crete." *Environmental Monitoring and Assessment* 149 (1-4): 19–28. doi:10.1007/s10661-008-0179-8.
- Kineke, G. C., Sternberg, R. W. 1992. "Measurements of High Concentration Suspended Sediments Using the Optical Backscatterance Sensor." *Marine Geology*. 108:253-258.
- Kirkby, M.J., B.J. Irvine, R.J.A. Jones, G. Govers, M. Boer, O. Cerdan, J. Daroussin, et al. 2008. "The PESERA Coarse Scale Erosion Model for Europe. I. - Model Rationale and Implementation." *European Journal of Soil Science* 59 (6): 1293–1306. doi:10.1111/j.1365-2389.2008.01072.x.

- Knight, J C, D Ball, and G N Robertson. 1991. "Analytical Inversion for Laser Diffraction Spectrometry Giving Improved Resolution and Accuracy in Size Distribution." *Applied Optics* 30 (33): 4795–99.
- Kourgialas, Nektarios N., George P. Karatzas, and Nikolaos P. Nikolaidis. 2010. "An Integrated Framework for the Hydrologic Simulation of a Complex Geomorphological River Basin." *Journal of Hydrology* 381 (3–4): 308–21. doi:10.1016/j.jhydrol.2009.12.003.
- Kurashige, Yoshimasa, and Yuichiro Fusejima. 1997. "Source Identification of Suspended Sediment from Grain-Size Distributions: I. Application of Nonparametric Statistical Tests." *CATENA* 31 (1–2): 39–52. doi:10.1016/S0341-8162(97)00033-7.
- Law, D. J., A. J. Bale, and S. E. Jones. 1997. "Adaptation of Focused Beam Reflectance Measurement to in-Situ Particle Sizing in Estuaries and Coastal Waters." *Marine Geology* 140 (1–2): 47–59. doi:10.1016/S0025-3227(97)00021-2.
- Lecce, Scott A. 2009. "A Depth-Proportional Intake Device for Automatic Water Samplers1." *JAWRA Journal of the American Water Resources Association* 45 (1): 272–77. doi:10.1111/j.1752-1688.2008.00269.x.
- Lenhart, T., A. Van Rompaey, A. Steegen, N. Fohrer, H.G. Frede, and G. Govers. 2005. "Condisering Spatial Distribution and Deposition of Sediment in Lumped and Semi-Distributed Models." *Hydrological Processes* 19 (3): 785–94. doi:10.1002/hyp.5616.
- Lewis, Jack. 1996. "Turbidity-Controlled Suspended Sediment Sampling for Runoff-Event Load Estimation." *Water Resources Research*, 2299–2310.
- Lewis, A. J., and Rasmussen, T. C. (1996). "A New, Passive Technique for the In Situ Measurement of Total Suspended Solids Concentrations in Surface Water." Technical Completion Report for Project # 14-08-001-G-2013 (07), U.S. Department of the Interior, Geological Survey. August 1996.
- Libicki, Charles, Keith W. Bedford, and James F. Lynch. 1989. "The Interpretation and Evaluation of a 3-MHz Acoustic Backscatter Device for Measuring Benthic Boundary Layer Sediment Dynamics." *The Journal of the Acoustical Society of America* 85 (4): 1501–11. doi:10.1121/1.397351.
- Littlewood, Ian G. 1992. "Estimating Contaminant Loads in Rivers: A Review". Publication - Report.

- Loch, R.J., Silburn, D.M., 1996. Constraints to sustainability – soil erosion. In: Clarke, L., Wylie, P.B. (Eds.), *Sustainable Crop Production in the Sub-tropics: an Australian Perspective*. QDPI.
- Lopes, T., J. Fallon, and T. Maluk. 2000. “Compositing Water Samples for Analysis of Volatile Organic Compounds.” *Journal of Environmental Engineering* 126 (8): 769–73. doi:10.1061/(ASCE)0733-9372(2000)126:8(769).
- Ludwig, K. A. and Hanes, D. M. 1990. “A Laboratory Evaluation of Optical Backscatterance Suspended Solids Sensors Exposed to Sand-Mud Mixtures.” *Marine Geology*. 94:173-179.
- Ludwig, W., and J.-L. Probst. 1998. “River Sediment Discharge to the Oceans: Present-Day Controls and Global Budgets.” *American Journal of Science* 298 (4): 265–95.
- McHenry, J. R., N. L. Coleman, J. C. Willis, A. C. Gill, O. W. Sansom, and B. R. Carroll. 1970. “Effect of Concentration Gradients on the Performance of a Nuclear Sediment Concentration Gage.” *Water Resources Research* 6 (2): 538–48. doi:10.1029/WR006i002p00538.
- Merritt, W. S., R. A. Letcher, and A. J. Jakeman. 2003. “A Review of Erosion and Sediment Transport Models.” *Environmental Modelling & Software* 18 (8–9): 761–99. doi:10.1016/S1364-8152(03)00078-1.
- Moraetis, D., D. Efstathiou, F. Stamati, O. Tzoraki, N.P. Nikolaidis, J.L. Schnoor, and K. Vozinakis. 2010. “High-Frequency Monitoring for the Identification of Hydrological and Bio-Geochemical Processes in a Mediterranean River Basin.” *Journal of Hydrology* 389 (1–2): 127–36. doi:10.1016/j.jhydrol.2010.05.037.
- Moriasi, DN, JG Arnold, MW Van Liew, RL Bingner, RD Harmel, and TL Veith. 2007. “Model Evaluation Guidelines for Systematic Quantification of Accuracy in Watershed Simulations.” *Transactions of the ASABE* 50 (3): 885–900.
- Nelson, M. E., P. C. Benedict, and American Society of Civil Engineers Hydraulics Division. 1950. *Measurement and Analysis of Suspended Sediment Loads in Streams*. American Society of Civil Engineers.
- Nikolaidis, N. P., F. Bouraoui, and G. Bidoglio. 2013. “Hydrologic and Geochemical Modeling of a Karstic Mediterranean Watershed.” *Journal of Hydrology* 477 (January): 129–38. doi:10.1016/j.jhydrol.2012.11.018.

- Novo, E.M.M., J.D. Hansom, and P.J. Curran. 1989. "The Effect of Viewing Geometry and Wavelength on the Relationship between Reflectance and Suspended Sediment Concentration." *International Journal of Remote Sensing* 10 (8): 1357–72. doi:10.1080/01431168908903973.
- Papadopoulos, J. and Ziegler, C. A. 1966. "Radioisotope Technique for Monitoring Sediment Concentration in Rivers and Streams." From: *Proc. on Radioisotope Instruments in Industry and Geophysics*. IAEA, Vienna, Austria. SM-68/26:pp. 381-394.
- Papanicolaou, T., A., M. Elhakeem, G. Krallis, S. Prakash, and J. Edinger. 2008. "Sediment Transport Modeling Review—Current and Future Developments." *Journal of Hydraulic Engineering* 134 (1): 1–14. doi:10.1061/(ASCE)0733-9429(2008)134:1(1).
- Pelletier, Jon D. 2012. "A Spatially Distributed Model for the Long-Term Suspended Sediment Discharge and Delivery Ratio of Drainage Basins." *Journal of Geophysical Research: Earth Surface* 117 (F2): F02028. doi:10.1029/2011JF002129.
- Phillips, J.M., and D.E. Walling. 1995. "Measurement in Situ of the Effective Particle-Size Characteristics of Fluvial Suspended Sediment by Means of a Field-Portable Laser Backscatter Probe: Some Preliminary Results." *Marine and Freshwater Research* 46 (1): 349–57.
- Potts, P. J., A. G. Tindle, and P. C. Webb. 1992. *Geochemical Reference Material Compositions: Rocks, Minerals, Sediments, Soils, Carbonates, Refractories & Ores Used in Research & Industry*. Latheronwheel, Caithness, U.K.; Boca Raton, FL: Whittles Pub. ; CRC Press.
- PSIAC, 1968. *Report of the Water Management Subcommittee on Factors Affecting Sediment Yield in the Pacific Southwest Area and Selection and Evaluation of Measures for Reduction of Erosion and Sediment Yield*. Pacific Southwest Inter-Agency Committee.
- Refsgaard, J. C.. 1997. "Parameterisation, Calibration and Validation of Distributed Hydrological Models." *Journal of Hydrology* 198 (1–4): 69–97. doi:10.1016/S0022-1694(96)03329-X.
- Reid, I., and L. E. Frostick. 1987. "Flow Dynamics and Suspended Sediment Properties in Arid Zone Flash Floods." *Hydrological Processes* 1 (3): 239–53. doi:10.1002/hyp.3360010303.

- Rijn, L. 1984. "Sediment Transport, Part II: Suspended Load Transport." *Journal of Hydraulic Engineering* 110 (11): 1613–41. doi:10.1061/(ASCE)0733-9429(1984)110:11(1613).
- Rijn, L. C. van, and A. S. Schaafsma. 1986. *Evaluation of Measuring Instruments for Suspended Sediment*. Waterloopkundig Lab.
- Riley, J. B., and Y. C. Agrawal. 1991. "Sampling and Inversion of Data in Diffraction Particle Sizing." *Applied Optics* 30 (33): 4800–4817. doi:10.1364/AO.30.004800.
- Ritchie, J. C. and Schiebe, F. R. 1986. "Monitoring Suspended Sediments with Remote Sensing Techniques." *Proceedings of workshop: "Hydrologic Applications of Space Technology."* IAHS publication no. 160.
- Rose, C. W. 1993. "Erosion and Sedimentation." In *Hydrology and Water Management in the Humid Tropics*. International Hydrology Series. Cambridge University Press.
- Roseen, R., T. Ballesteros, G. Fowler, Q. Guo, and J. Houle. 2011. "Sediment Monitoring Bias by Automatic Sampler in Comparison with Large Volume Sampling for Parking Lot Runoff." *Journal of Irrigation and Drainage Engineering* 137 (4): 251–57. doi:10.1061/(ASCE)IR.1943-4774.0000168.
- Salkield, A. P., LeGood, G. P., and Soulsby, R. L. 1981. "Impact Sensor for Measuring Suspended Sand Concentration." *Conference On Electronics for Ocean Technology*, Birmingham, England.
- Schat, Jan. 1997. "Multifrequency Acoustic Measurement of Concentration and Grain Size of Suspended Sand in Water." *The Journal of the Acoustical Society of America* 101 (1): 209–17. doi:10.1121/1.418003.
- Sibetheros, I. A., S. Nerantzaki, D. Efstathiou, G. Giannakis, and N. P. Nikolaidis. 2013. "Sediment Transport in the Koiliaris River of Crete." *Procedia Technology* 8: 315–23. doi:10.1016/j.protcy.2013.11.042.
- Skinner, J. V., Federal Inter-Agency Sedimentation Project (U.S.), United States Interagency Advisory Committee on Water Data Subcommittee on Sedimentation, Geological Survey (U.S.), and United States Army Corps of Engineers. 1989. *Model-B Sediment-Concentration Gage: Factors Influencing Its Readings and a Formula for Correcting Its Errors*. U.S. Army Engineer District.

Stewart, B. A., United States Agricultural Research Service, and United States Environmental Protection Agency Office of Research and Development. 1976. Control of Water Pollution from Cropland. Dept. of Agriculture, Agricultural Research Service.

Strahler, A. H., and A. N. Strahler. 2006. *Introducing Physical Geography*. J. Wiley.

Subcommittee, Pacific Southwest Inter-agency Committee Water Management. 1968. Report of the Water Management Subcommittee on Factors Affecting Sediment Yield in the Pacific Southwest Area and Selection and Evaluation of Measures for Reduction of Erosion and Sediment Yield.

Syvitski, J.P.M., and J.D. Milliman. 2007. "Geology, Geography, and Humans Battle for Dominance over the Delivery of Fluvial Sediment to the Coastal Ocean." *Journal of Geology* 115 (1): 1–19. doi:10.1086/509246.

Syvitski, J.P.M., S.D. Peckham, R. Hilberman, and T. Mulder. 2003. "Predicting the Terrestrial Flux of Sediment to the Global Ocean: A Planetary Perspective." *Sedimentary Geology* 162 (1-2): 5–24. doi:10.1016/S0037-0738(03)00232-X.

Syvitski, J.P.M., C.J. Vörösmarty, A.J. Kettner, and P. Green. 2005. "Impact of Humans on the Flux of Terrestrial Sediment to the Global Coastal Ocean." *Science* 308 (5720): 376–80. doi:10.1126/science.1109454.

Syvitski, J.P.M., and J.D. Milliman. 2007. "Geology, Geography, and Humans Battle for Dominance over the Delivery of Fluvial Sediment to the Coastal Ocean." *The Journal of Geology* 115 (1): 1–19. doi:10.1086/509246.

Tazioli, G.S. "Nuclear Techniques for Measuring Sediment Transport in Natural Streams — Examples from Instrumented Basins."

Theurer, F., Clarke, C.D., 1991. Wash load component for sediment yield modeling. Proceedings of the Fifth Federal Interagency Sedimentation Conference. Interagency Advisory Committee on Water Data, Subcommittee on Sedimentation (pp. 7-1 7-8).

Thomas, R. B., Pacific Southwest Forest, Range Experiment Station, and Forest Service. 1985. "Estimating Total Suspended Sediment Yield with Probability Sampling." *Water Resources Research*, 1381–88.

Thorne, P. D, C. E Vincent, P. J Hardcastle, S Rehman, and N Pearson. 1991. "Measuring Suspended Sediment Concentrations Using Acoustic Backscatter Devices." *Marine Geology* 98 (1): 7–16. doi:10.1016/0025-3227(91)90031-X.

- Thorne, Peter D., Kendall R. Waters, and Terry J. Brudner. 1995. "Acoustic Measurements of Scattering by Objects of Irregular Shape." *The Journal of the Acoustical Society of America* 97 (1): 242–51. doi:10.1121/1.413109.
- Tzoraki, O., and N.P. Nikolaidis. 2007. "A Generalized Framework for Modeling the Hydrologic and Biogeochemical Response of a Mediterranean Temporary River Basin." *Journal of Hydrology* 346 (3–4): 112–21. doi:10.1016/j.jhydrol.2007.08.025.
- Tzoraki, O., N.P. Nikolaidis, Y. Amaxidis, and N.T. Skoulikidis. 2007. "In-Stream Biogeochemical Processes of a Temporary River." *Environmental Science & Technology* 41 (4): 1225–31. doi:10.1021/es062193h.
- Van Oost, K., G. Govers, and P. Desmet. 2000. "Evaluating the Effects of Changes in Landscape Structure on Soil Erosion by Water and Tillage." *Landscape Ecology* 15 (6): 577–89. doi:10.1023/A:1008198215674.
- Van Rompaey, A.J.J., G. Verstraeten, K. Van Oost, G. Govers, and J. Poesen. 2001. "Modelling Mean Annual Sediment Yield Using a Distributed Approach." *Earth Surface Processes and Landforms* 26 (11): 1221–36. doi:10.1002/esp.275.
- Verstraeten, G., J. Poesen, Joris de Vente, and X. Koninckx. 2003. "Sediment Yield Variability in Spain: A Quantitative and Semiquantitative Analysis Using Reservoir Sedimentation Rates." *Geomorphology* 50 (4): 327–48. doi:10.1016/S0169-555X(02)00220-9.
- Verstraeten, G., K. Van Oost, A. Van Rompaey, J. Poesen, and G. Govers. 2002. "Evaluating an Integrated Approach to Catchment Management to Reduce Soil Loss and Sediment Pollution through Modelling." *Soil Use and Management* 18 (4): 386–94. doi:10.1079/SUM2002150.
- Walling, D. E., and Arthur J. Horowitz. 2005. *Sediment Budgets*. IAHS Press.
- Welch, Norman H., and Paul B. Allen. 1973. "Field Calibration and Evaluation of a Nuclear Sediment Gage." *Water Resources Research* 9 (1): 154–58. doi:10.1029/WR009i001p00154.
- Wheater, H.S., Jakeman, A.J., Beven, K.J., 1993. Progress and directions in rainfall-runoff modelling. In: Jakeman, A.J., Beck, M.B., McAleer, M.J. (Eds.), *Modelling Change in Environmental Systems*. John Wiley and Sons, Chichester, pp. 101–132
- Williams, J.R. 1975. *Sediment Yield Prediction with Universal Equation Using Runoff Energy Factor*. Agricultural Research Service ARS-S-40. USDA.

- Wischmeier, W.H., and D.D. Smith. 1978. *Predicting Rainfall Erosion Losses: A Guide to Conservation Planning*. Science and Education Administration, U.S. Department of Agriculture.
- Wisser, D., B. M. Fekete, C. J. Vörösmarty, and A. H. Schumann. 2010. "Reconstructing 20th Century Global Hydrography: A Contribution to the Global Terrestrial Network-Hydrology (GTN-H)." *Hydrol. Earth Syst. Sci.* 14 (1): 1–24. doi:10.5194/hess-14-1-2010.
- Witt, W. and S. Rüthele. 1996. "Laser Diffraction – Unlimited?" *Particle & Particle Systems Characterization* 13 (5): 280–86. doi:10.1002/ppsc.19960130505.
- Wren, D.G., Barkdoll, B.D., Kuhnle, R.A., and Derrow, R.W. 2000. "Field techniques of suspended sediment measurement". *Journal of Hydraulic Engineering*. 126(2): 97-104.
- Yang, X. 2003. *Manual on Sediment Management and Measurement*. Secretariat of the World Meteorological Organization.
- Young, R.A., J.T. Merrill, T.L. Clarke, and J.R. Proni. 1982. "Acoustic Profiling of Suspended Sediments in the Marine Bottom Boundary Layer." *Geophysical Research Letters* 9 (3): 175–78. doi:10.1029/GL009i003p00175.
- Xu, J.P. 1997. "Converting Near Bottom OBS Measurements into Suspended Sediment Concentrations." *Geo-Marine Letters*. 17:154-161.